



TITLE:

# Light Control of the Tet Gene Expression System in Mammalian Cells

AUTHOR(S):

Yamada, Mayumi; Suzuki, Yusuke; Nagasaki, Shinji C.; Okuno, Hiroyuki; Imayoshi, Itaru

---

CITATION:

Yamada, Mayumi ...[et al]. Light Control of the Tet Gene Expression System in Mammalian Cells. Cell Reports 2018, 25(2): 487-500.e6

ISSUE DATE:

2018-10-09

URL:

<http://hdl.handle.net/2433/234704>

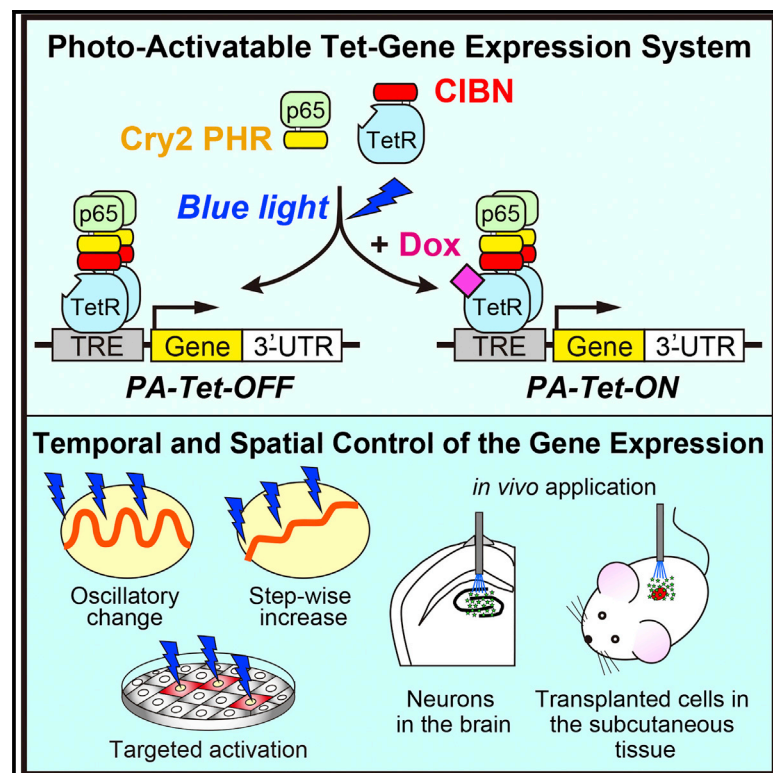
RIGHT:

© 2018 The Author(s). This is an open access article under the CC BY-NC-ND license (<http://creativecommons.org/licenses/by-nc-nd/4.0/>).

# Cell Reports

## Light Control of the Tet Gene Expression System in Mammalian Cells

### Graphical Abstract



### Authors

Mayumi Yamada, Yusuke Suzuki,  
Shinji C. Nagasaki, Hiroyuki Okuno,  
Itaru Imayoshi

### Correspondence

imayoshi.itaru.2n@kyoto-u.ac.jp

### In Brief

Yamada et al. develop photoactivatable (PA)-Tet-OFF/ON systems for precise temporal and spatial control of cellular gene expression. The PA-Tet-OFF/ON can be applied to various cell types *in vitro* and *in vivo*, and their transcriptional activities are tightly regulated by blue light illumination and the small molecule Dox.

### Highlights

- Photoactivatable (PA)-Tet-OFF/ON systems are developed in mammalian cells
- The PA-Tet-OFF/ON activities are dually controlled by blue light and Dox
- The PA-Tet-OFF/ON allows precise temporal and spatial control of gene expression
- The PA-Tet-OFF/ON can be applied to various cell types *in vitro* and *in vivo*



# Light Control of the Tet Gene Expression System in Mammalian Cells

Mayumi Yamada,<sup>1,2,3,4</sup> Yusuke Suzuki,<sup>1,2,4</sup> Shinji C. Nagasaki,<sup>1</sup> Hiroyuki Okuno,<sup>2,3,4,5</sup> and Itaru Imayoshi<sup>1,2,3,6,7,8,\*</sup>

<sup>1</sup>Research Center for Dynamic Living Systems, Graduate School of Biostudies, Kyoto University, Kyoto 606-8501, Japan

<sup>2</sup>Institute for Frontier Life and Medical Sciences, Kyoto University, Kyoto 606-8507, Japan

<sup>3</sup>World Premier International Research Center Initiative, Institute for Integrated Cell-Material Sciences, Kyoto University, Kyoto 606-8501, Japan

<sup>4</sup>Medical Innovation Center/SK Project, Graduate School of Medicine, Kyoto University, Kyoto 606-8507, Japan

<sup>5</sup>Graduate School of Medical and Dental Sciences, Kagoshima University, Kagoshima 890-8544, Japan

<sup>6</sup>The Hakubi Center for Advanced Research, Kyoto University, Kyoto 606-8302, Japan

<sup>7</sup>Precursory Research for Embryonic Science and Technology, Japan Science and Technology Agency, Saitama 332-0012, Japan

<sup>8</sup>Lead Contact

\*Correspondence: [imayoshi.itaru.2n@kyoto-u.ac.jp](mailto:imayoshi.itaru.2n@kyoto-u.ac.jp)

<https://doi.org/10.1016/j.celrep.2018.09.026>

## SUMMARY

Gene expression and its network structure are dynamically altered in multicellular systems during morphological, functional, and pathological changes. To precisely analyze the functional roles of dynamic gene expression changes, tools that manipulate gene expression at fine spatiotemporal resolution are needed. The tetracycline (Tet)-controlled gene expression system is a reliable drug-inducible method, and it is used widely in many mammalian cultured cells and model organisms. Here, we develop a photoactivatable (PA)-Tet-OFF/ON system for precise temporal control of gene expression at single-cell resolution. By integrating the cryptochrome 2-cryptochrome-interacting basic helix-loop-helix 1 (Cry2-CIB1) light-inducible binding switch, expression of the gene of interest is tightly regulated under the control of light illumination and drug application in our PA-Tet-OFF/ON system. This system has a large dynamic range of downstream gene expression and rapid activation/deactivation kinetics. We also demonstrate the optogenetic regulation of exogenous gene expression *in vivo*, such as in developing and adult mouse brains.

## INTRODUCTION

Optogenetics, a method by which genetically encoded light-sensitive proteins are used to regulate the behavior of living cells and organisms, has emerged during the past decade (Kim et al., 2017; Repina et al., 2017; Rost et al., 2017). Optogenetics has been mainly applied in neuroscience, in which light-mediated activation of microbial opsins depolarizes or polarizes neuronal membranes, subsequently inducing temporally precise

activation or inhibition of targeted neuronal cells. Most of these optogenetic tools are based on light-sensitive ion channels or transporters (Deisseroth, 2015; Rajasethupathy et al., 2016; Song and Knöpfel, 2016). By applying other types of photoactivatable (PA) molecules, such as light-switchable enzymes or protein interaction modules, the application of optogenetic tools has expanded to studies of the regulation of various cellular functions, including cell signaling, subcellular localization, and gene expression (Aoki et al., 2017; Giordano et al., 2013; Kennedy et al., 2010; Konermann et al., 2013; Maiuri et al., 2015; Repina et al., 2017).

Optogenetic tools that can control cellular gene expression have been developed, which have the potential to overcome the technical limitations of conventional chemically regulated gene expression systems (Crefcoeur et al., 2013; Hallett et al., 2016; Hörner et al., 2017; Imayoshi et al., 2013; Konermann et al., 2013; Liu et al., 2012a; Motta-Mena et al., 2014; Müller et al., 2013b; Pathak et al., 2017; Polstein and Gersbach, 2012; Shimizu-Sato et al., 2002; Wang et al., 2012; Yazawa et al., 2009). Rapid and dynamic changes of gene expression patterns (e.g., oscillatory changes or stepwise increases) are difficult to address using classical gene expression regulation methods, such as chemically regulated systems, due to their poor temporal and highly invasive characteristics.

The Tet-OFF/ON system is the most commonly used chemically regulated system in mammalian cells (Das et al., 2016; Gossen and Bujard, 1992). In this system, treatment with a small molecule (i.e., tetracycline [Tet] or doxycycline [Dox], a more stable Tet analog) regulates exogenous gene expression in genetically targeted cell populations. The Tet-OFF system activates downstream gene expression in the absence of Dox, whereas the Tet-ON system activates it in the presence of Dox. The original Tet system has been improved significantly for use in eukaryotic cells, including mammalian cells.

The latest version of the Tet-OFF/ON system tightly controls gene expression, with low background and high maximum gene expression levels. However, the system has several drawbacks, such as limited reversibility and poor spatial control due



to diffusion of the regulator molecule Dox in the culture medium or the body of model organisms. For instance, because Dox can bind to cells or the extracellular matrix, highly invasive procedures, such as multiple washes or replating of cells, are required to completely remove the Dox compound (Das et al., 2016). This inherent limitation excludes experiments requiring rapid activation or deactivation of the gene of interest, such as dynamic gene expression changes in stem or progenitor cells during differentiation, or circadian or ultradian rhythm studies of clock genes. Spatial control of the Tet system is challenging, and manipulation of targeted cells or cell populations is difficult; even activated caged Dox may diffuse from the irradiated regions (Cambridge et al., 2009). Therefore, there is an increasing demand for the development of a light-inducible Tet-OFF/ON system for the precise temporal and spatial control of cellular gene expression.

We designed a blue light-inducible Tet gene expression system based on the concept of split transcription factors, in which light-dependent interactions between PA-protein interaction modules can reconstitute a split DNA-binding domain and transcription activation domain. We exploited the *Arabidopsis thaliana*-derived blue light-responsive heterodimer formation module consisting of the cryptochrome 2 (Cry2) photoreceptor and its specific binding protein cryptochrome-interacting basic helix-loop-helix 1 (CIB1) (Wu and Yang, 2010; Yu et al., 2010). *Arabidopsis* Cry2 is a photolyase-like photoreceptor that regulates the development and growth of plants via circadian clock regulation. Cry2 has two domains: an N-terminal photolyase homology region (PHR) and a cryptochrome C-terminal extension (CCE or CCT). PHR is the chromophore-binding domain that binds noncovalently to the chromophore flavin adenine dinucleotide (FAD). Cry2 can bind to the basic helix-loop-helix (bHLH) transcription factor CIB1 in a blue light-specific manner. It was shown that truncated versions of Cry2 and CIB1 essential domains act as blue light-dependent heterodimer formation modules, and several point mutations of Cry2 induce faster or slower photocycles (Kennedy et al., 2010; Liu et al., 2012a; Taslimi et al., 2016).

The optimized PA-Tet-OFF/ON system has a large dynamic range of downstream gene expression, rapid activation, and deactivation kinetics. The PA-Tet-OFF/ON system can be tightly regulated by Dox treatment like the original Tet system; this allows for precise dual light and drug control of the amount, timing, and pattern of downstream gene expression. Finally, we demonstrate the light control of gene expression *in vivo*, such as in the developing and adult mouse brain and the subcutaneous tissue.

## RESULTS

### Functional Screening of Optimized PA-Tet-OFF Transcription Factors

We aimed to optimize the PA-Tet gene expression system in mammalian cells. Most light-inducible gene expression systems were established in yeast cells. Some light-inducible gene expression systems optimized in yeast cells do not work efficiently in mammalian cells (Pathak et al., 2017; unpublished data). Therefore, we conducted functional screenings of candi-

date constructs in the immortalized human embryonic kidney cell line HEK293T (Figures 1, S1, and S2; Tables S1, S2, S3, S4, and S5). We used the DNA binding, dimerization, and Tet-binding domains of Tet repressor (TetR) (residues 1–206) as the split DNA-binding domain, and the transcription activation domain of p65 (p65 AD). In mammalian cells, p65 AD induces greater gene expression compared with other transcription activating domains, such as virus protein 16 (VP16) (Wang et al., 2012). In addition to the Cry2-CIB1 system, we also performed functional screenings of PA-Tet-OFF constructs using other optical dimer formation systems, such as tunable light-controlled interacting protein tags (TULIPs) (Strickland et al., 2012), original light-inducible dimer/improved light-inducible dimer (oLID/iLID) (Guntas et al., 2015; Hallett et al., 2016), Vivid (VVD), and Magnet (Kawano et al., 2015; Wang et al., 2012). However, not all constructs showed efficient light-dependent transcriptional activity (data not shown). Therefore, we focused on PA-Tet constructs consisting of the Cry2-CIB1 system (Figures 1A and S1).

Co-expressed full-length versions of *Arabidopsis* Cry2 and CIB1 act as transcriptional regulators in other model organisms, and the truncated version of Cry2/CIB1 is sufficient to mediate blue light-dependent interactions with diminished activity of the original transcriptional regulation (Hughes et al., 2012; Kennedy et al., 2010; Liu et al., 2012a; Taslimi et al., 2016). Detailed characterization of truncated or mutated Cry2/CIB1 was performed by the Tucker lab and others, and binding affinity, kinetics, and background activity were found to differ among Cry2/CIB1 variants and their applied pairs. In addition, the configuration of Cry2/CIB1 (i.e., N- or C-terminal fusion) in the fused constructs affects the activity of the reconstituted constructs. Therefore, we rigorously investigated the following parameters: (1) Cry2/CIB1 truncation and point mutations, (2) Cry2/CIB1 configuration, (3) Cry2/CIB1 codon usage, (4) TetR point mutations, (5) linker sequences between TetR and Cry2/CIB1, and (6) expression vector structures necessary for efficient expression in target cells.

In the first set of screened constructs, we fused TetR (residues 1–206) to the N terminus of Cry2 or its derivatives. However, we did not observe apparent light-induced gene expression in either case when CIB1 and its derivatives were fused to the N terminus or C terminus of p65 AD (Figures S1A–S1D; Tables S1 and S2). This may be due to the nuclear clearing phenotype of Cry2-tethered proteins (Pathak et al., 2017). When Cry2 is fused to certain nuclear-localized proteins having internal dimerization domains, the fused proteins are redistributed outside the nuclei in a light-dependent manner. Some Cry2-fused transcription factors undergo substantial nuclear protein clearing upon illumination, resulting in light-dependent loss of protein function (Pathak et al., 2017). It was reported that the nuclear clearing phenotype was dependent on the presence of a dimerization domain contained within Cry2-fused proteins, and TetR has an inherent dimerization domain. Therefore, we next tried to validate the constructs in which TetR was fused to the N terminus of CIB1 or its derivatives. Some construct pairs showed light-dependent transcriptional activity, but the induced and background gene levels varied among them (Figures S1A, S1B, S1E, and S1F; Tables S3 and S4).

We selected the T86 construct pair for subsequent validations and designated it PA-Tet-OFF because of its low levels of



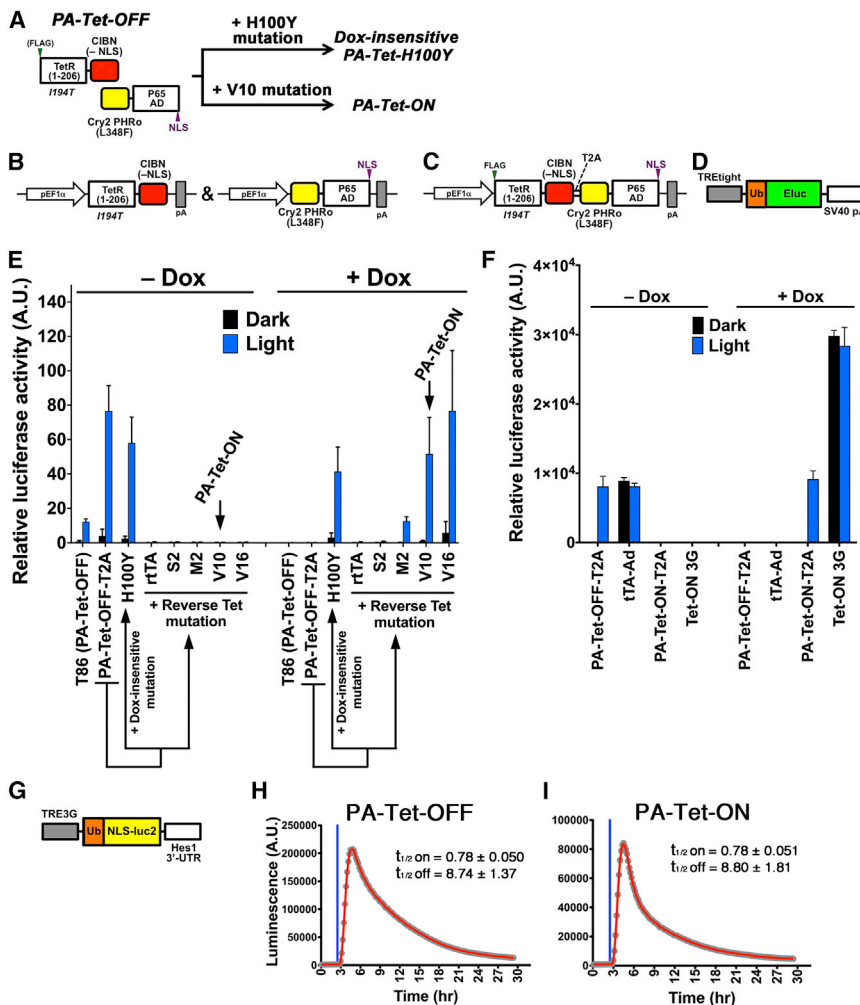


### Figure 1. Generation of the Photoactivatable (PA)-Tet-OFF/ON System

(A) Schematic illustration of the PA-Tet-OFF construct and generation of the doxycycline (Dox)-insensitive PA-Tet-H100Y and PA-Tet-ON construct. Cry2 PHRo indicates the N-terminal photolyase homology region (PHR) of mammalian codon-optimized Cry2. CIBN indicates a truncated version of mammalian codon-optimized CIB1 lacking the conserved bHLH domain, which mediates dimerization and DNA binding. See also [Figure S1](#). (B and C) Schematics of PA-Tet-OFF expression vectors of the two expression plasmids (B) and the single expression plasmid with T2A self-cleaving peptide sequence (C).

(D) TREtight-Ub-Eluc reporter was used for the construct screening and validation.

(E) Validation of light- and Dox-dependent regulation of the PA-Tet-OFF/ON system in transiently transfected HEK293T cells. Dox (75 ng/mL) was supplied in the cell culture medium. The PA-Tet-H100Y and PA-Tet-ON constructs were derived from the PA-Tet-OFF construct having the T2A sequence.

(F) Comparison between the PA-Tet-OFF/ON and the original chemically regulated Tet-OFF/ON systems. Illumination with blue light pulses was extended to 36 hr. A total of 500 ng/mL Dox was added to the cell culture medium. The data represent means  $\pm$  SDs ( $n = 3$ ) from one experiment, and experiments were repeated three times, with similar results. See also [Tables S5 and S6](#).

(G–I) Temporal characteristics of the PA-Tet-OFF (H) and PA-Tet-ON (I). The reporter construct consisting of TRE3G, Ub-NLS-luc2, and Hes1 3' UTR sequences was transiently transfected to HEK293T cells (G) Dox (1,000 ng/mL) was supplied in the cell culture medium (I). A single blue light pulse was applied, and the half-lives of the switch-on/-off kinetics were estimated. The timing of blue light exposure is indicated by the vertical blue lines. Experiments were repeated at least three times, with similar results.

background activity under dark conditions and consistent light-induced gene expression (Figure 1). Although other construct pairs, such as T53, T57, or T63, also yielded significantly increased downstream gene expression on prolonged illumination, which was applied in construct functional screening, these construct pairs showed very low levels of downstream gene expression under a limited number of blue light pulses (data not shown). In contrast, the T86 PA-Tet-OFF construct showed a rapid and large increase of downstream gene expression, even after a single blue light pulse (Figures 1G and 1H). The TetR-CIB81 fused constructs (T65–T70) showed high levels of downstream gene expression; however, their transcriptional activity was significantly leaky (Table S3).

In the construct screening experiments, photomodule-fused TetR and p65 AD were expressed separately from the two independent plasmid vectors. When the PA-Tet-OFF construct was expressed by a single plasmid vector, in which the photomodule-fused TetR and p65 AD were co-expressed together with a T2A self-cleaving peptide (Kim et al., 2011), the light-induced

expression levels were preserved or increased (Figures 1C, 1E, and 1F). This may be due to the improved simultaneous expression of the photomodule-fused TetR and p65 AD in each transfected cell.

We used TetR with an I194T mutation and an SPKKK linker sequence in the PA-Tet-OFF constructs. This SPKKK linker sequence, which is a part of the nuclear localization signal (NLS) of SV40 T antigen, was originally used in the TetR-Krüppel associated box (KRAB) construct (Szulc et al., 2006). During the initial phase of construct screening, we noticed that application of the TetR I194T mutation and SPKKK linker sequence resulted in superior performance compared with TetR wild-type or other amino acid substitution constructs with typical flexible linker sequences (Figure S2). Neither transcriptional activity nor Dox regulation was affected by introducing the I194T mutation into the original Tet transcription factors (i.e., Tet-OFF Advanced or Tet-ON 3G Systems; data not shown), indicating that the TetR I194T mutation was effective only in our PA-Tet system.

### Generation of PA-Tet-ON Transcription Factors

The Tet-OFF system activates downstream gene expression in the absence of Dox, whereas the Tet-ON system activates it in the presence of Dox. Historically, random mutational studies and phenotypic screenings in *Escherichia coli*, *Saccharomyces cerevisiae*, and virus evolution in human cells revealed that some amino acid substitutions of TetR led to reverse TetR function: binding to the tetracycline response element (TRE or TetO) sequence in the presence but not the absence of Dox. We applied these reverse phenotype mutations, rtTA (E71K, D95N, L101S, G102D), S2 (E19G, A56P, D148E, H179R), M2 (S12G, E19G, A56P, D148E, H179R), V10 (E19G, A56P, F67S, F86Y, D148E, R171K, H179R), or V16 (V9I, E19G, A56P, F67S, F86Y, D148E, R171K, H179R) (Das et al., 2016) to the PA-Tet-OFF, and validated their Dox-dependent transcriptional activity (Figures 1A and 1E). We also generated PA-Tet constructs with the Dox-insensitive H100Y mutation (Hecht et al., 1993).

As expected, the blue light-dependent transcriptional activity of PA-Tet-OFF was abolished in the presence of Dox; conversely, PA-Tet (H100Y) was not affected by Dox treatment (Figure 1E; Table S5). Each PA-Tet-ON construct with differing sets of point mutations had different induced-gene expression levels and background activity in the presence of Dox. Among them, we selected a PA-Tet-ON construct with the V10-mutation due to these high light-induced gene expression levels and low background activity in the dark.

Taken together, the data show blue light-inducible transcription of selected PA-Tet-OFF/ON constructs can be controlled by Dox (Figure 1E). In the candidate construct screenings of the PA-Tet-OFF/ON system, the cells were exposed to pulsed blue light (e.g., 2-s pulse every 1 min) for only 3 hr before cell lysis. When cells were exposed to similar blue light pulses (1-s pulse every 30 s) for longer time periods (e.g., 36 hr), the induced luciferase reporter activity for PA-Tet-OFF/ON was dramatically increased and essentially similar to the chemically regulated Tet-OFF/ON systems (Figure 1F; Table S6).

Cry2 is rapidly activated by light illumination and then spontaneously dissociates from CIB1, with a half-life of ~5.5 min (Kennedy et al., 2010; Taslimi et al., 2016). The fast activation and deactivation kinetics of the Cry2-CIB1 system may allow for dynamic changes to the downstream gene expression in the PA-Tet-OFF/ON system. To address this point, we used the destabilized luciferase reporter Ub-NLS-luc2 (Figure 1G) and placed the Hes1 3' untranslated region (UTR) sequence just downstream of Ub-luc, which is known to induce a shorter mRNA half-life, to prevent accumulation of the reporter activities in cells (Luker et al., 2003; Voon et al., 2005; Masamizu et al., 2006). When cells transfected with the PA-Tet-OFF/ON and TRE3G-Ub-NLS-luc2 reporter constructs were exposed to a 1-min short pulse of blue light, transient expression of the luciferase reporter was observed, indicating the temporally dynamic control of downstream gene expression in the PA-Tet system (Figures 1H and 1I).

### Detailed Characterization of PA-Tet-OFF/ON

To reduce experimental variability caused by different cellular transfection efficiencies, we used lentivirus vectors to stably ex-

press PA-Tet-OFF/ON in mouse mammary gland epithelial Eph4 cells, and generated single-cell-derived clones (Figures 2A–2C). Consistent with the PA-Tet-OFF/ON transient transfection data, luciferase reporter activity was greatly enhanced in the stable PA-Tet-OFF/ON cells illuminated with blue light relative to cells left in the dark. The light-inducible ability of stable clones was preserved over a long period of time (i.e., at least several months under standard cell culture conditions). These results indicate that the PA-Tet-OFF/ON system can generate reliable light-induced gene expression in both transiently and stably incorporated cells.

One major advantage of a light-inducible gene expression system is the ease of tuning gene expression levels by adjusting illumination protocols. We investigated the effects of modifying light intensity on induced-gene expression levels in the PA-Tet-OFF/ON system. For example, we observed an expected light intensity-dependent increase in reporter activity in PA-Tet-OFF transduced Eph4 cells (Figure 2D). PA-Tet transcriptional activity was activated in cells even under weak blue light exposure ( $1.7 \text{ W/m}^2$ ), indicating the high sensitivity of this system.

Compared with other light-controlled gene expression systems, one unique feature of the PA-Tet-OFF/ON system is its susceptibility to drug control. We investigated the effects of Dox concentration on light-induced gene expression levels (Figures 2E and 2F). As expected, Dox attenuated light-induced gene expression in a concentration-dependent manner in the PA-Tet-OFF system (Figure 2E). Conversely, light-induced gene expression was increased in correlation with the Dox concentration in the Tet-ON system between 0 and 250 ng/mL (Figure 2F). At Dox concentrations >250 ng/mL, the induced luciferase activity was slightly decreased; however, the Dox concentration for maximum gene expression depends on the cell type and gene delivery method. In the case of Eph4 cells transduced with the PA-Tet-ON system by lentivirus vectors, higher luciferase activity was observed at 500 ng/mL than at 250 ng/mL of Dox (Figures 2G–2I). Notably, drug treatment effects were observed in both systems at very low Dox concentrations: 1 ng/mL in the PA-Tet-OFF system and 10 ng/mL in the PA-Tet-ON system (Figures 2E and 2F). Furthermore, downstream gene expression was precisely controlled by changing the light intensity and drug concentration. Because PA-Tet-ON activity did not change in direct proportion to light intensity or Dox concentration, it was difficult to precisely control the PA-Tet activity at the intermediate level by modifying a single parameter. However, by creating a matrix of light intensity and Dox concentration, we could induce the desired reporter gene expression levels (Figures 2G–2I). For instance, variable reporter genes levels were induced (range, 0- to 50-fold) when the light energy delivered varied from 0 to  $7.1 \text{ W/m}^2$  and the Dox concentration varied from 0 to 500 ng/mL in the PA-Tet-ON-Eph4 cells. This dual-control feature of the PA-Tet-OFF/ON system will contribute to systems biology experiments, in which gene expression levels must be tightly controlled.

The ability to control the PA-gene expression system via drug treatment is important for ordinary cell culture maintenance and light irradiation-priming experiments. Most PA-gene expression systems are activated with low amounts of light; therefore, short exposure to room lighting is sufficient to activate transcriptional

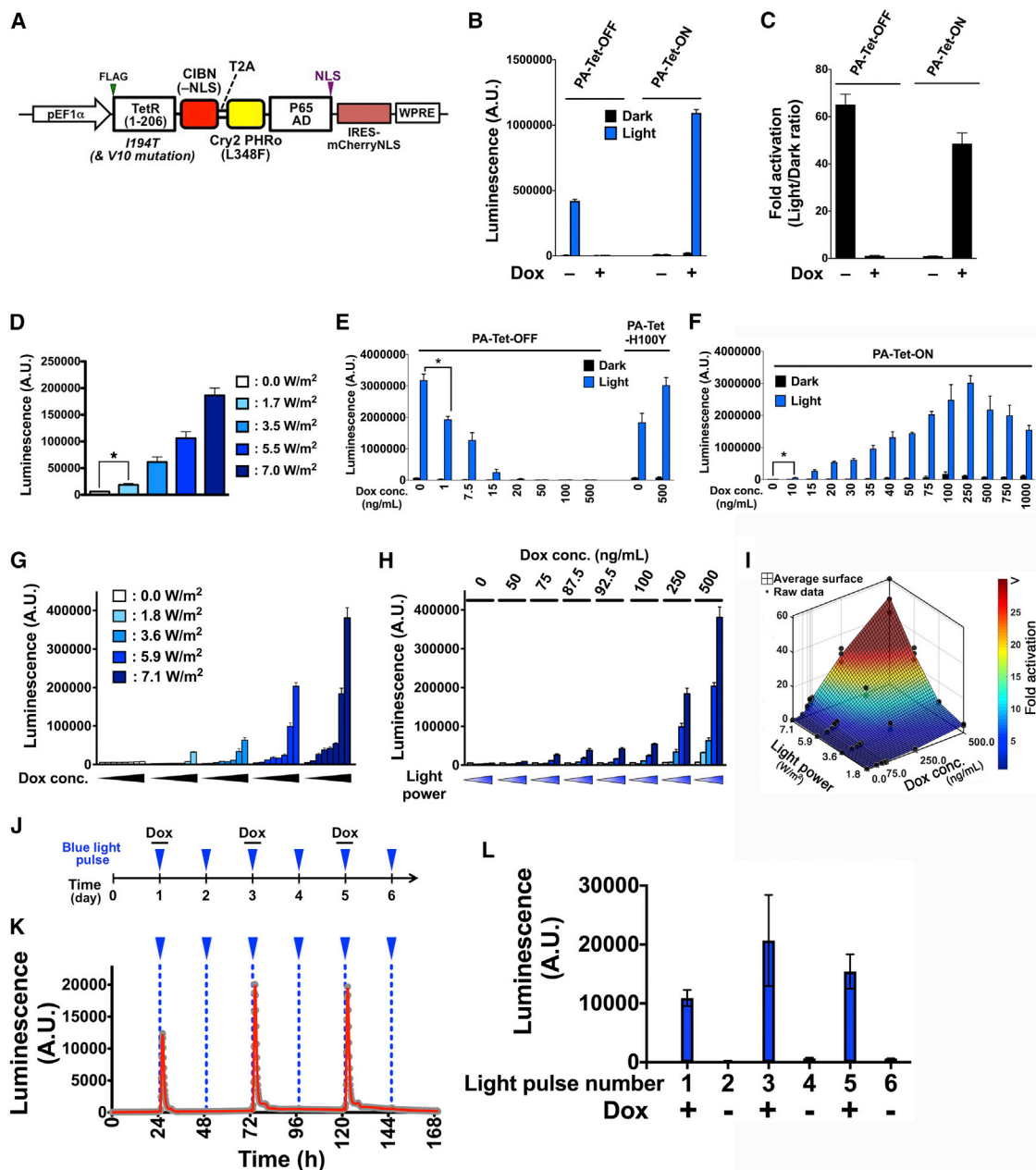


**Figure 2. Light- and Dox-Dependent Regulation of the PA-Tet System**

(A–C) Validation of Dox- and light-dependent regulation of the PA-Tet-OFF/ON system in Eph4 cells stably transduced with lentivirus vectors (A). Dox (1,000 ng/mL) was supplied in the cell culture medium (B and C).

(D) Blue light intensity-dependent transcriptional activity of the PA-Tet-OFF system in Eph4 cells stably transduced with lentivirus vectors.

(E and F) Dox concentration-dependent transcriptional activity of the PA-Tet-OFF (E) and PA-Tet-ON system (F) in transiently transfected HEK293T cells.

(G–I) Blue light intensity- and Dox concentration-dependent transcriptional activity of the PA-Tet-ON system in Eph4 cells stably transduced with lentivirus vectors. The radiant energy varied from 0 to 7.1 W/m². Dox concentration varied from 0 to 500 ng/mL. The same dataset is differently expressed in the three panels.

(J–L) Conditional activation of light-dependent transcriptional activity of the PA-Tet-ON system in long-term cell culture. Schematic design of the experiment (J). Dox (1,000 ng/mL) was added to the medium on days 1, 3, and 5 (K). Transcriptional activity was activated by blue light exposure only with Dox treatment in the stably transduced Eph4 cells (L). The timing of blue light exposure is indicated by arrowheads and dotted blue lines.

The data represent means ± SDs (n = 3) from one experiment, and experiments were repeated twice, with comparable results. \*p < 0.05; two-tailed Student's t test.

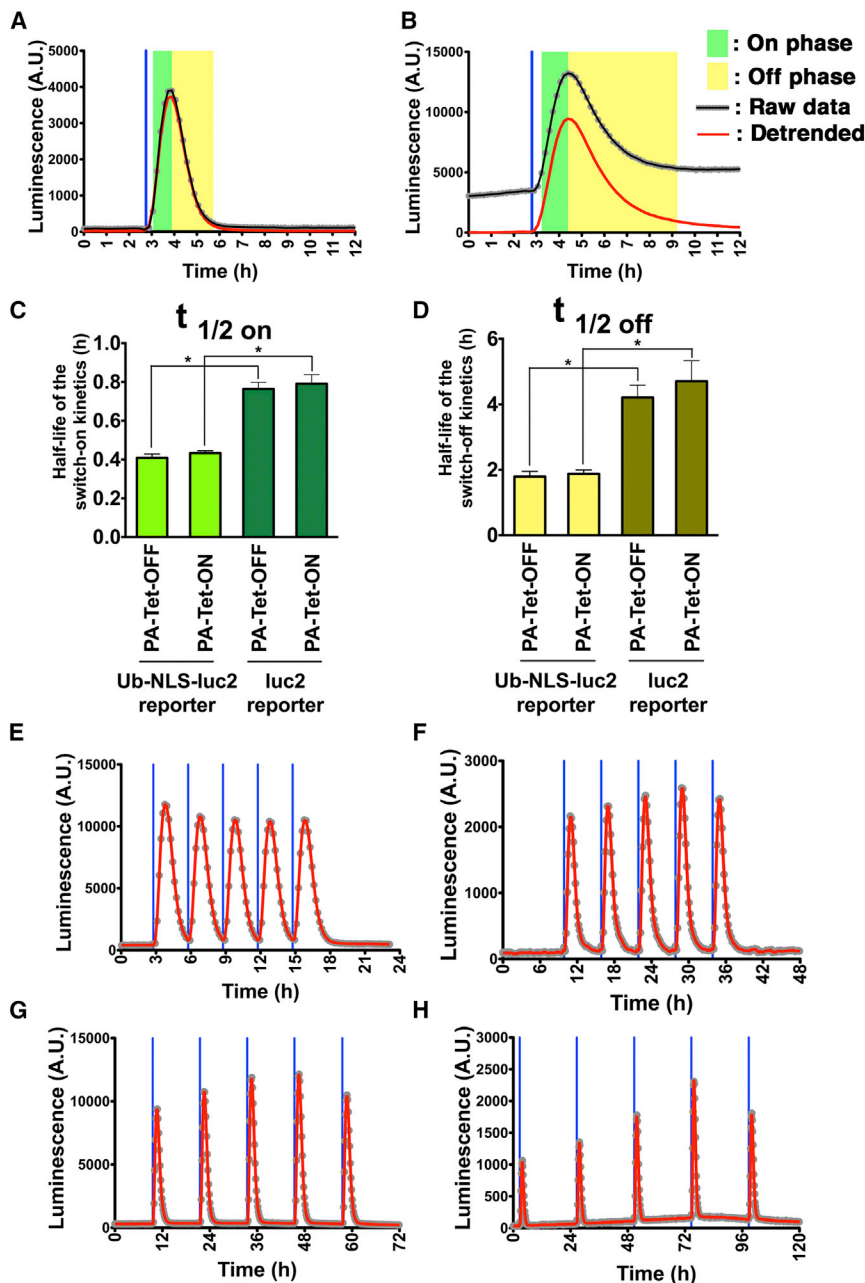


**Figure 3. Temporal Regulation of the PA-Tet System**

(A and B) The PA-Tet-OFF-transduced Eph4 cells with lentivirus vectors were exposed to a single blue light pulse. Reporter constructs consisted of TRE3G, Ub-NLS-luc2, and Hes1 3' UTR sequences (A) or TRE3G, luc2, and Hes1 3' UTR sequences (B). The timing of blue light exposure is indicated by vertical blue lines.

(C and D) Using the single light pulse dataset, kymograph analysis was used to determine the half-lives of the switch on (C)/off (D) kinetics of light-induced gene expression in the PA-Tet-OFF/ON systems. The data represent means  $\pm$  SDs ( $n \geq 6$ , each condition).

(E–H) Periodic activation of the PA-Tet-OFF-system induced oscillatory expression of the downstream reporter gene. Reporter constructs consisted of TRE3G, Ub-NLS-luc2, and Hes1 3' UTR sequences. PA-Tet-OFF-transduced Eph4 cells were repeatedly exposed to blue light pulses with 3- (E), 6- (F), 12- (G), or 24-hr (H) intervals.

Experiments were repeated at least three times, with similar results. \* $p < 0.05$ ; two-tailed Student's  $t$  test.

ducing Dox just before illumination (Figures 2J–2L). Therefore, drug control of the PA-Tet system can eliminate undesired gene induction, particularly in long-term experiments.

### Temporal Features of the PA-Tet-OFF/ON System

Because of the rapid activation and deactivation kinetics of the Cry2-CIB1 switch, the PA-Tet-OFF/ON system can be applied for dynamic control of downstream gene expression. We validated the temporal characteristics of PA-Tet constructs by applying short pulses of light (1 or 2 min) and monitored the luciferase expression level, which was under the control of TRE sequences, in real time. When we analyzed stable cell clones transduced with PA-Tet-OFF/ON and TRE3G-Ub-NLS-luc2 reporter, peak blue light pulse-induced

activity (Imayoshi et al., 2013; Pathak et al., 2014; Wang et al., 2012). Therefore, cells with the blue light-inducible gene expression system must be consistently maintained under absolute darkness or specialized red or far-red light equipment. In addition, cells must be primed under dark conditions before the start of the light irradiation experiments, which can take several hours or days. In contrast, the light-dependent activity of the PA-Tet-OFF/ON system can be conditionally induced by drug exposure or washout. For instance, in the PA-Tet-ON system, light-dependent gene expression did not persist in the absence of Dox; conversely, light-dependent gene expression was induced during the course of the 1-week experiment by intro-

ducing Dox just before illumination (Figures 2J–2L). Therefore, drug control of the PA-Tet system can eliminate undesired gene induction, particularly in long-term experiments. When we periodically applied blue light pulses with different periods, robust oscillatory expression was induced at 3, 6, 12, and 24 hr (Figures 3E–3H). Accumulated Ub-NLS-luc2 reporter expression was not observed, even in the rapid periodic activation experiment (e.g., 3-hr period). The destabilized luciferase reporter with the short half-life-3' UTR sequence was essential for rapid ultradian rhythm generation. Conversely, normal, stable luciferase reporters may be suitable for periodic gene expression experiments during a longer period, mimicking the expression of typical clock genes during the circadian period. The activation



and deactivation kinetics of light-induced gene expression in the PA-Tet system were extended when a reporter construct with normal, stable luciferase was used (Figures 3B–3D).

One major advantage of the PA gene expression system is the possibility of systematic design of downstream gene expression dynamics at fine temporal resolution. If we applied different luciferase reporter constructs with longer reporter protein and mRNA degradation half-lives, such as Ub-Eluc with SV40 pA sequences, then different reporter expression dynamics were induced by the same light illumination protocols (Figure S3). For example, a continuous increase in luciferase activity was observed under blue light irradiation with a 3-hr period (Figures S3B–S3D). Conversely, a stepwise increase in luciferase activity was observed with 6- or 12-hr periodic illumination (Figure S3E–S3J). Thus, by changing the reporter protein and mRNA half-lives, as well as the light exposure pattern, various gene expression patterns (e.g., oscillatory change, continuous increase, stepwise increase) can be designed using the PA-Tet system.

In the PA-Tet-OFF/ON/H100Y constructs, a Cry2 PHR module with the L348F slow photocycle mutation (~24-min half-life) was integrated (Taslimi et al., 2016), but we observed no apparent differences in the switch on/off kinetics relative to other candidate constructs having the wild-type Cry2 PHR, such as the T63 construct. We also tested the Cry2 W349R fast photocycle mutation, but introduction of this mutation abolished the light-induced activity of both PA-Tet-OFF/ON/H100Y constructs (data not shown).

### Targeted Activation of the PA-Tet System in Spatially Restricted Cells

Another major advantage of a light-controlled system is the ability to spatially restrict gene expression in targeted cells. To characterize such spatially restricted gene expression in targeted cells, we equipped a bioluminescence imaging microscope with a digital mirror device (DMD) to generate spatial patterns of light. After exposure to a blue light pulse, bioluminescence imaging revealed that luciferase expression in PA-Tet-OFF-transduced Eph4 cells with the TRE3G-Ub-NLS-luc2 reporter occurred in the shape determined by the DMD device (Figure 4). For instance, different round-shaped cell populations were sequentially activated at different times (Figures 4A–4C; Video S1). Furthermore, successful targeted activation of single cells was observed (Figures 4D and 4E). When 10 targeted cells were illuminated simultaneously, specific light-induced reporter expression was observed in the targeted cells, but not in the surrounding unilluminated cells. Our drug-controllable PA-Tet-OFF/ON system provides an experimental platform to systematically manipulate gene expression over a large dynamic range with fine temporal resolution at the single-cell level.

### Validation of the PA-Tet System in Primary Cultured Tissues and Cells

We examined the capability of the PA-Tet system to induce light-triggered gene expression in the primary cultured cells and tissues. We tested PA-Tet activity in neural stem or progenitor cells of the developing mouse brain (Figures 5A–5D). We introduced the PA-Tet-OFF expression plasmid with the TRE3G-Ub-NLS-

luc2 reporter into neural stem or progenitor cells via *ex utero* electroporation. When acute tissue slices derived from the electroporated brain were periodically illuminated, wave-like reporter expression was observed in the ventricular/subventricular zone (VZ/SVZ), where the neural stem or progenitor cells divide and produce neurons (Imayoshi and Kageyama, 2014a, 2014b).

We then introduced the PA-Tet system into differentiated neurons with adeno-associated virus (AAV) vectors. Due to the size limitation of the AAV vector, we generated two AAV vectors; one expressing the TetR (1–206)-CIBN (without NLS) fusion construct and mCherryNLS, and the other the NLS-attached Cry2 PHR (L348F)-p65 AD fusion construct (Figure 5E). We co-transduced the PA-Tet-OFF/ON AAV vectors into cultured primary neurons derived from the hippocampus of mouse pups (Figures 5F and 5G). We observed efficient expression of the transduction marker, mCherryNLS, in MAP2<sup>+</sup> (microtubule-associated protein 2<sup>+</sup>) neurons. We also introduced the TRE3G-Ub-NLS-luc2 reporter lentivirus into AAV-transduced neurons. When these neurons were periodically irradiated with blue light in a 3-hr period, robust oscillatory expression of the destabilized luciferase was observed (Figures 5H–5J). These results document that the PA-Tet system can be introduced into cells by various methods, including electroporation and use of AAV vectors. We also demonstrated efficient light-triggered gene expression in primary cultured cells, such as neural stem or progenitor cells of acutely prepared embryonic brain slices and dissociated neurons from the developing hippocampus.

### In Vivo Application of the PA-Tet System

We also validated light- and Dox-mediated gene expression control in the intact living mouse. First, we transduced PA-Tet-OFF AAV vectors (Figure 5E) into hippocampal neurons of adult TRE-GFP transgenic mice (Figures 6A and 6B). As reported previously, leaky expression of GFP in this transgenic mouse strain was very limited (Figure 6C) (Sano and Yokoi, 2007). For the hippocampus-light illumination, awake and freely moving mice were stimulated using a blue light-emitting diode (LED) connected to the optical implant via fiber patch cables and a rotary joint at an intensity of 85.6 W/m<sup>2</sup>, duty cycle of 1.6% (1-s pulses at 0.016 Hz) for 12 hr (Figure 6B). We found that 42.8% ± 2.3% of the CA1 neurons and 36.7% ± 6.0% of the granule cells of the dentate gyrus (DG) were GFP<sup>+</sup>. In contrast, when not illuminated, only 4.7% ± 1.4% of the CA1 neurons and 4.4% ± 1.6% of the DG neurons expressed GFP (Figures 6C and 6D), indicating successful blue light-dependent gene expression control by the PA-Tet-OFF system in the adult brain.

Second, we analyzed Dox-dependent suppression of the transcriptional activity by the PA-Tet-OFF system in neurons of the brain. In this experiment, the TRE3G-luc2 reporter AAV vector was used for the quantitative analysis of light-gated gene expression (Figure 6E). Mice were mounted and fixed on the custom-made stage, and transduction marker mCherry-expressing regions of the brain were exposed to blue light via optical fibers at an intensity of 40 W/m<sup>2</sup>, duty cycle of 7.1% (1-s pulses at 0.071 Hz) for 3 hr (Figures 6F and 6G). As expected, when Dox was administered at a dose of 0.1 mg/g body weight



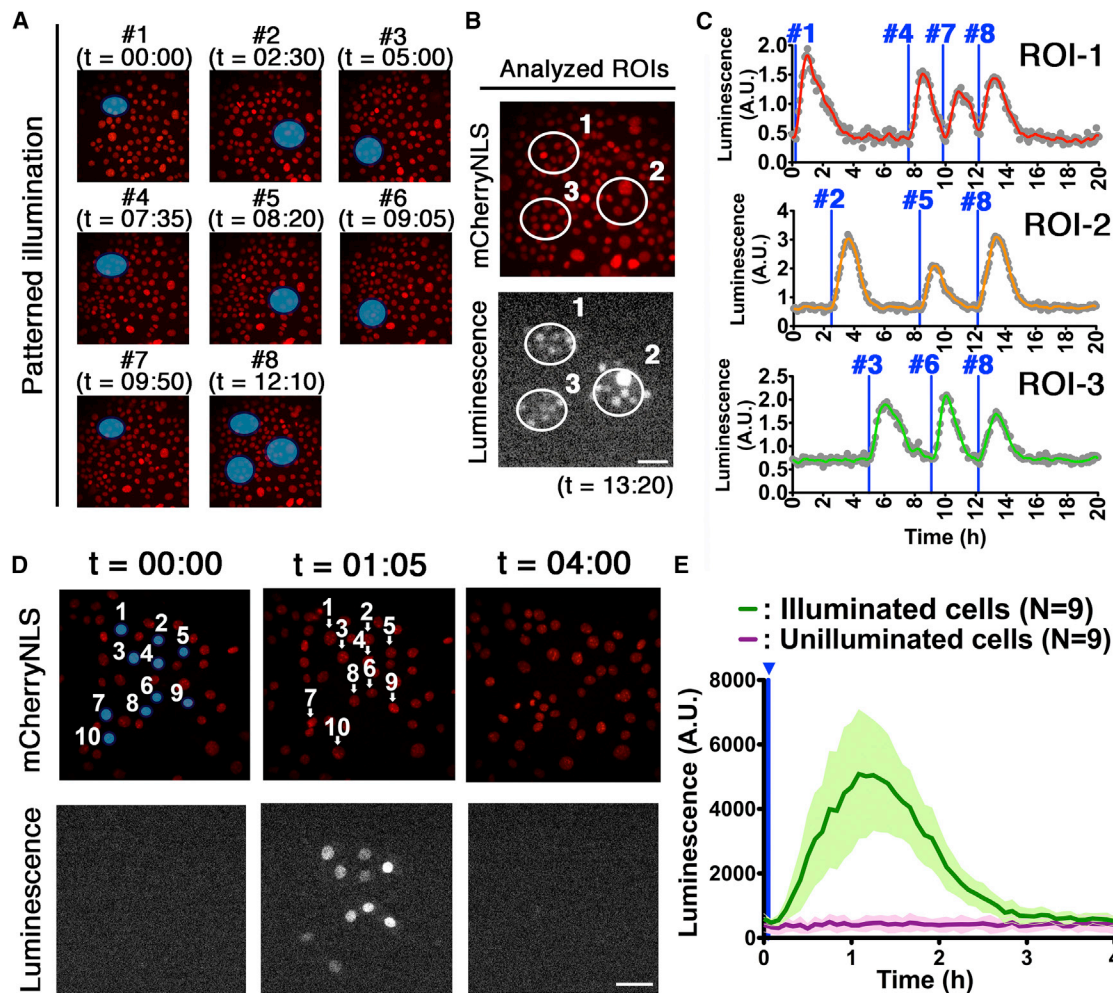


**Figure 4. Spatially Controlled Regulation of the PA-Tet System via Patterned Light Illumination**

(A–C) Targeted cell populations were illuminated by patterned light generated by a digital mirror device (DMD). The patterned light, indicated by blue circles, was applied at different time points to Eph4 cells in which the PA-Tet-OFF system was stably transduced with lentivirus vectors. The timing is indicated in hr and min (A). Light-induced reporter expression was analyzed in three regions of interest (ROIs) (B) and quantified (C). The timing of blue light illumination is indicated by vertical blue lines.

(D and E) The patterned light was applied to 10 targeted cells (cells 1–10) simultaneously, and their light-induced reporter expression was monitored (D). (E) The light-induced luciferase activity was upregulated only in illuminated cells (green) but not in adjacent unilluminated cells (magenta) (E). The reporter activity of the illuminated cells was quantified, except for cell 9 because it divided during the time-lapse imaging experiment. The surrounding unilluminated cells were randomly selected and quantified.

The data represent means  $\pm$  SDs ( $n = 9$ ) from one experiment. Experiments were repeated at least three times, with similar results. Scale bars, 12.5  $\mu$ m for (A), (B), and (D).

1 hr before illumination, light-induced luciferase activity was reduced to the background level seen in the dark (Figure 6H). We also observed the opposite effects of Dox in PA-Tet-ON AAV-injected brains. Blue light-dependent transcription was only observed in the presence of Dox (Figure 6I). In these experiments, light-induced gene expression levels were lower compared with the *in vitro* experiments using the HEK293T and Eph4 cell lines and primary cultured neurons. This is probably because the illuminated blue light with the optical fibers was exposed to the limited population of transduced neurons in the brain. Although the PA-Tet and reporter AAVs were broadly transduced to the neurons of the brain, the neurons

near the tip of the optical fiber were exposed to the strong blue light. For inducing gene expressions in broadly scattered neurons in the brain, other types of light source, such as sheet-type LEDs, could be more efficient.

We next analyzed the recovery of light-inducible transcription activity of the PA-Tet-OFF after Dox removal (Figure 6J). Suppression of light-induced luciferase expression was maintained for 4 days after Dox removal. However, it increased to the original level seen without Dox treatment on washout day 5 (Figure 6K). These data indicate that the effects of Dox lasted for approximately 4 days in the mouse pup brains. This documents the suitability of conditional light-gated activation of the PA-Tet-OFF

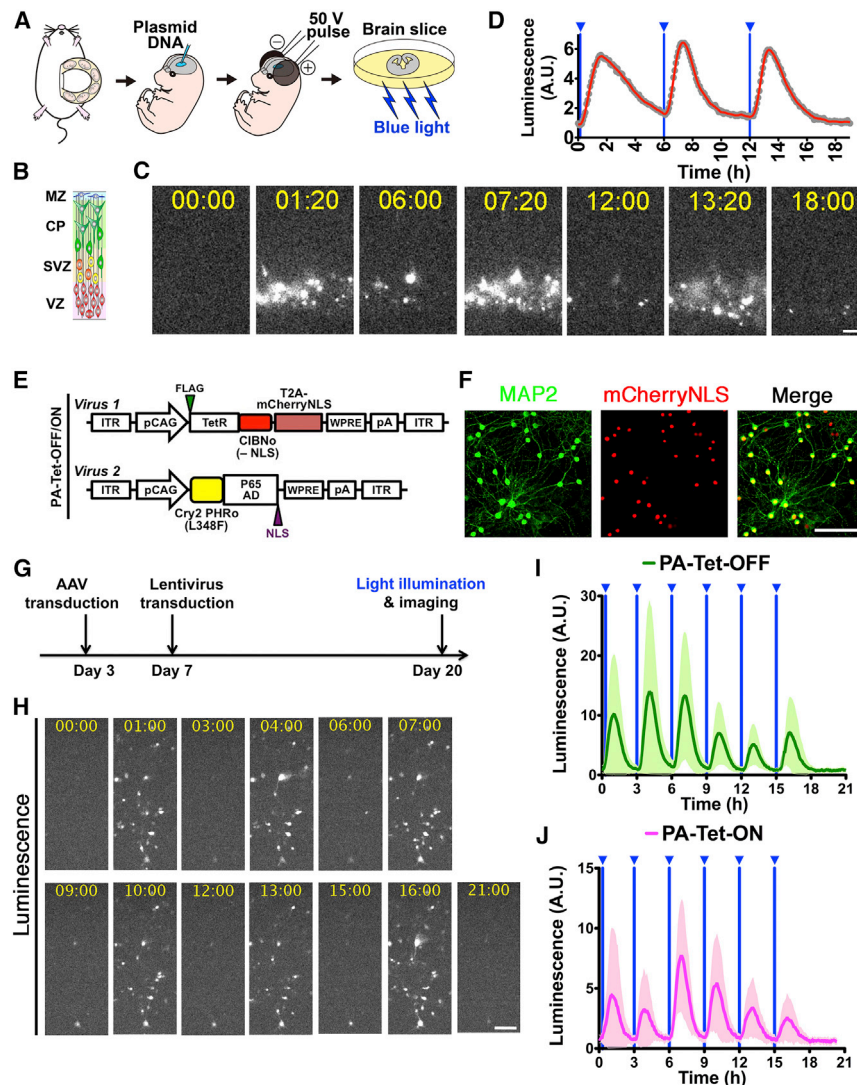


**Figure 5. Optogenetic Manipulation of Gene Expression in the Primary Cultured Tissues and Cells**

(A–D) The PA-Tet-OFF system was introduced into neural stem or progenitor cells of the developing brain by *ex utero* electroporation. The electroporated brain was immediately extracted from the embryo and sliced on tissue culture membrane (A). (B–D) Blue light was periodically applied to the slice during a 6-hr period, and reporter activity was monitored (B and C). Blue light-induced luciferase expression was observed in the neural stem or progenitor cells of the ventricular and subventricular zone (VZ/SVZ) (C and D).

(E–G) Cultured neurons derived from the mouse hippocampus were transduced with AAV vectors expressing the PA-Tet system (E) and the TRE3G-Ub-NLS-luc2-Hes1 3' UTR reporter lentivirus vector. Most of the MAP2<sup>+</sup> (microtubule-associated protein 2<sup>+</sup>) neurons expressed the AAV transduction marker mCherryNLS (F). The experimental schedule is illustrated in (G).

(H–J) Periodic activation of transcription in the transduced neurons, in which the PA-Tet-OFF (H and I) or PA-Tet-ON (J) system was induced. The cultured neurons were repeatedly exposed to blue light pulses with 3-hr intervals. The timing of blue light exposure is indicated by vertical blue lines. Dox (500 ng/mL) was added to activate the PA-Tet-ON constructs. The reporter activity of the 25 (I) and 13 (J) illuminated cells was quantified.

The data represent means  $\pm$  SDs. Experiments were repeated twice, with similar results. Scale bars, 25  $\mu$ m for (C) and (H) and 100  $\mu$ m for (F). MZ, marginal zone; CP, cortical plate.

## DISCUSSION

Here, we describe an inducible gene expression system that can be dually controlled by exposure to blue light and by specific drug application in various

mammalian cells. We developed the PA-Tet-OFF/ON system for precise temporal control of cellular gene expression at single-cell resolution. Previously, we adopted the PA-Gal4/UAS (upstream activation sequence) system, in which the PA transcription factor was GAVPO, to analyze the functional importance of gene expression changes of the bHLH transcription factor *Ascl1* in the regulation of neural stem cells (Imayoshi et al., 2013; Imayoshi and Kageyama, 2014a, 2014b). Because VVD, the smallest light-oxygen-voltage domain-containing protein, is used as a photocontrolled dimer-formation module and GAVPO is very small (56 kDa), it can be expressed in multiple cell types via various gene delivery methods, including lipofection and electroporation of expression plasmids, and viral vectors, such as lentivirus vectors (Imayoshi et al., 2013; Isomura et al., 2017; Wang et al., 2012). GAVPO is extremely sensitive to light, and brief pulses of weak blue light are sufficient to induce high expression levels of the downstream genes. Consequently, GAVPO has some technical limitations, such as undesired downstream gene expression. When GAVPO is expressed in

system for use during a narrow time window, depending on systemic Dox treatment to prevent undesired activation outside the experimental schedule.

Finally, we assessed light-inducible gene expression of the PA-Tet-OFF system in subcutaneous tissue to demonstrate the broad utility of this tool also outside the brain. The PA-Tet-OFF-transduced Eph4 cells with lentivirus vectors (Figures 2A–2C) were engrafted into the subcutaneous tissue of adult mouse back skin (Figures S4A and S4B). The engrafted regions of anesthetized mice were then illuminated with blue light (200 W/m<sup>2</sup>, 1 min). Dynamic changes in luciferase signals were imaged by a charge-coupled device (CCD) camera. The luciferase reporter activity was observed only in the blue light-exposed mice without Dox but not in the non-irradiated mice (Figures S4B–S4D). These results indicated that efficient and reliable optogenetic regulation of exogenous gene expression can be achieved *in vivo* (e.g., developing brain, adult brain, and subcutaneous tissue in mice) using the PA-Tet system.

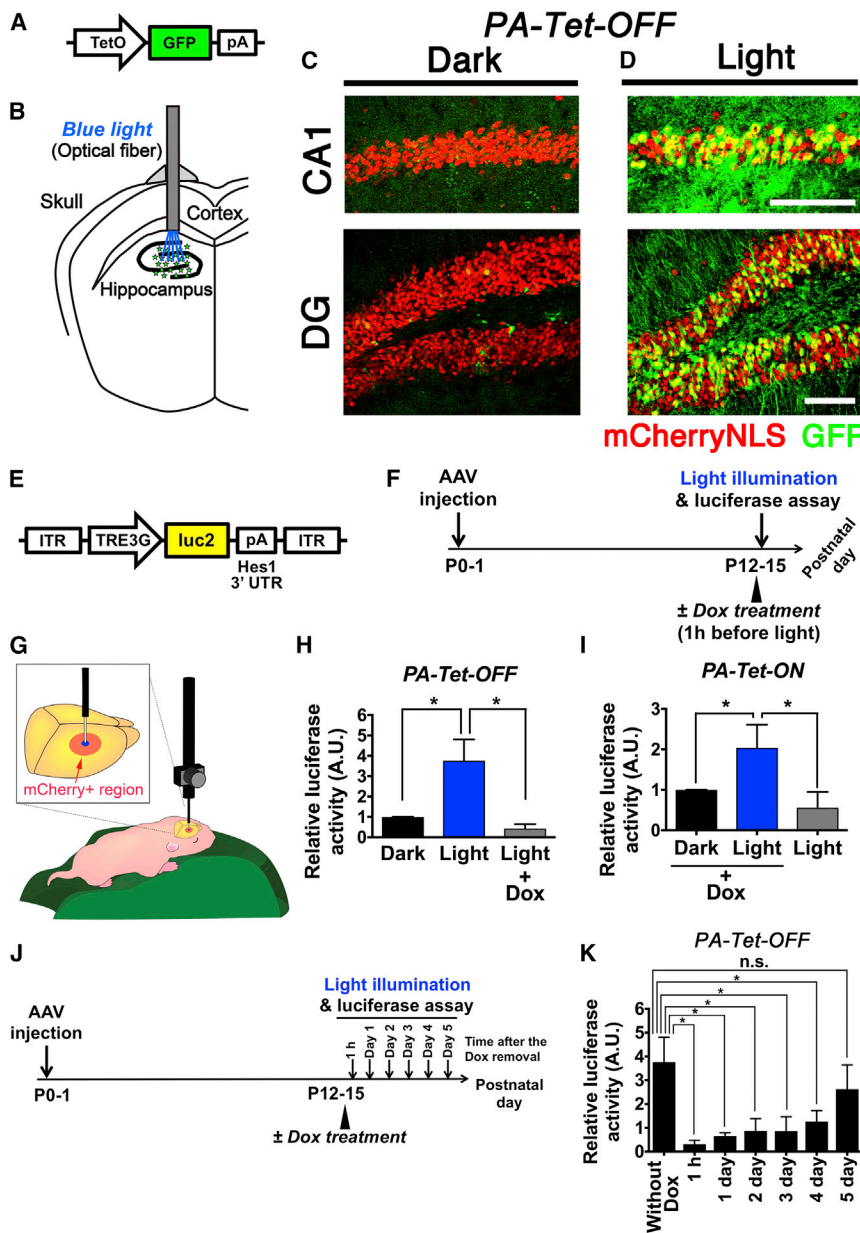


### Figure 6. Optogenetic Manipulation of Gene Expression in the Brain

(A–D) Light-induced gene expression in hippocampus-neurons of the adult mouse brain. Schematic illustration of the TetO-GFP transgenic reporter mouse line (A) and illumination of the AAV-transduced hippocampal neurons by optical fiber (B). The brains were examined 12 hr after the initiation of illumination.

(C and D) GFP reporter expression was increased in the neurons of the hippocampal CA1 and dentate gyrus (DG) regions in a blue light-dependent manner (D), but not in a dark manner (C). Experiments were repeated at least three times, with similar results.

(E–K) Light- and Dox-dependent gene expression in the brain of mouse pups. TRE3G-luc2-Hes1 3' UTR AAV vector was used as the transcription reporter (E). At 12–15 days after AAV injections, blue light illumination was started, and its effects were assessed. Dox was given 1 hr before exposure to light (F).

(G) Schematic illustration of illumination of the AAV-transduced neurons in the brain of mouse pups by optical fiber. In PA-Tet-OFF AAV-transduced brains, luciferase activity was significantly increased in a blue light-dependent manner, but this light-induced transcription was repressed in the presence of Dox (H).

(H and I) In contrast, in the PA-Tet-ON AAV-transduced brains, light-dependent transcription was induced only in the presence of Dox but not without it (I). Luminescence data were normalized to that of dark (H) and dark + Dox (I).

(J) Experimental schedule of the conditional light-induced gene expression with the PA-Tet-OFF by transient Dox administration. After the single injection of Dox, light-induced transcriptional activity was tested at the indicated time points.

(K) The suppressive effects mediated by Dox on the blue light-dependent transcription of the PA-Tet-OFF lasted for 4 days, but they disappeared on washout day 5. Luciferase assay data in the dark of each condition were used for the correction of data in the light of the same condition.

The data represent means  $\pm$  SDs ( $n \geq 3$ , each condition). Scale bars, 100  $\mu$ m. \* $p < 0.05$ ; two-tailed Student's *t* test.

cells at a high level, significant leaky transcriptional activity is observed, even in the dark (Ma et al., 2013; Wang et al., 2012; unpublished data). Furthermore, GAVPO and most of the other PA-gene expression systems are activated by low levels of light, and short exposure to room light is sufficient to activate transcriptional activity. Therefore, it cannot be used under normal room lighting conditions without being activated. More important, application of the Gal4/UAS system is not commonly used in the study of mammalian cells or organisms, likely due to the toxicity of the Gal4 transcription activator and the ease of chromatin silencing in the UAS sequence in mammalian cells, especially in transgenic animals (Habets et al., 2003). Therefore, development of an efficient and reliable PA gene expression sys-

tem that can be widely used in mammalian cells and model animals (e.g., the PA-Tet-OFF/ON system) is desirable.

There are no reports to date of an efficient blue light-inducible PA-Tet-OFF/ON system. To meet this need, a red/far-red light-controlled Tet system using the *Arabidopsis*-derived phytochrome interaction factor 6 (PIF6)-phytochrome B (PhyB) optical dimer system was developed (Müller et al., 2013a). For this system to work, phyB must bind with a chromophore, phytychromobilin, or phycocyanobilin (PCB); however, these molecules are not endogenous in yeast or mammalian cells (Pathak et al., 2014; Uda et al., 2017). Therefore, mammalian cells must be supplied with PCB for this system to act as an efficient red/far-red light-controlled gene switch. This requirement is problematic



for light-inducible gene expression *in vivo*. Recently, a near-infrared light-activatable Tet-gene expression system was developed (Kaberniuk et al., 2016). In this system, a bacterial phytochrome-based BphP1-PpsR2 optical dimer module was adapted. A large dynamic range of downstream gene expression was induced in a near-infrared-dependent manner both in cultured mammalian cells and deep tissues of mice *in vivo*. BphP1 uses biliverdin, which is endogenously present in mammalian cells, as its chromophore. Thus, there is no need to supply any exogenous chromophore to the cell culture medium or to animals *in vivo* in the BphP1-PpsR2-based gene expression system. However, these systems have longer deactivation times. Single-pulse light illumination can sustain sufficient transgene expression for ~20 hr, potentially inhibiting application of these systems to the precise functional analysis of rapid and dynamic gene expression changes.

Other than these optogenetic gene expression-regulation tools, many light-inducible gene expression systems have been developed by adapting different PA molecules (Crefcoeur et al., 2013; Hallett et al., 2016; Hörner et al., 2017; Konermann et al., 2013; Liu et al., 2012a; Motta-Mena et al., 2014; Müller et al., 2013b; Pathak et al., 2017; Polstein and Gersbach, 2012; Shimizu-Sato et al., 2002; Yazawa et al., 2009; Hisatomi and Furuya, 2015; Nguyen et al., 2018; Wang et al., 2017). These include light-mediated control of exogenous (e.g., Gal4/UAS, LexA, Tet, EL222, Cre-mediated switch) and endogenous (e.g., nuclease-dead Cas9 [dCas9], TAL effector [TALE], zinc-finger transcription factor) gene expression. Some systems were also designed to be controlled by both light and the state of the specific cell-signaling molecules (Wang et al., 2017).

It was expected that these systems would be applied for fine gene expression control *in vivo*. However, for such *in vivo* use, higher standards are required in terms of sensitivity, dynamic range, maximum gene expression level, and background activity level. To reduce the effects of phototoxicity resulting from exposure to intense light, high sensitivity is essential for developing transcription control systems using lower power light. In general, the PA molecules adapted for use in light-controlled transcription factors do have very high sensitivity to light. Therefore, relatively low light power, typically 10- to 100-fold less than is used for the activation of ChR2, is sufficient for light-induced gene expression. However, the dynamic range and maximum gene expression levels are not very high in most light-inducible gene expression systems, resulting in limited downstream gene expression, even on continuous or multiple illuminations. More important, most light-inducible gene expression systems are inherently leaky in the unilluminated condition. This could be caused by the leaky nature of the PA-transcription factors or their binding site containing promoters. Also, a too-high sensitivity to light could cause undesired leaky gene expression at ambient light levels. Compared with *in vitro* experiments, fine control of the activity of light-inducible gene expression systems is more difficult *in vivo*. For instance, in experiments using single-cell-derived clones under the same conditions of light-controlled gene expression, very rigorous light-mediated control can be achieved *in vitro*, whereas in *in vivo* experiments, most cells in the tissues are heterogeneous in terms of the levels of

expression of PA-transcription factors and/or copy number and status of the target elements. Therefore, light-inducible gene expression systems having high sensitivity, large dynamic range, and low background activity are needed for reliable light-inducible gene expression control *in vivo*.

In addition, for the *in vivo* use of light-inducible gene expression systems, gene silencing is also problematic, especially for long-term experiments. For example, the UAS sequence of the Gal4/UAS system is highly susceptible to transcriptional silencing by epigenetic changes. The light-activatable LexA and EL222 systems have not been proven to be effective in *in vivo* mammalian models (Pathak et al., 2014; Motta-Mena et al., 2014).

PA-Cre systems are effective *in vivo*, such as in rodent brain and liver, but Cre-mediated conditional gene expression systems only provide permanent gene expression and do not allow control of reversal (Taslimi et al., 2016; Kawano et al., 2016). Furthermore, satisfactory suppression of leaky recombination in the dark but efficient activation on illumination is very difficult to achieve. In addition, the gene delivery method for light-inducible gene expression systems is another issue to be considered. For example, PA-dCas9 is a very powerful tool for the optical control of endogenous genes, but, in addition to the PA-dCas9, a constant supply of the guide RNAs is also needed (Nihongaki et al., 2015, 2017). Co-introduction of multiple genetic components is more difficult for *in vivo* experiments than for *in vitro* experiments. Some light-inducible gene expression systems are combined with drug use for achieving tighter control. However, increasing the number of components constituting the gene expression system prevents efficient *in vivo* delivery.

Recently, synthetic transcription factors activated by light under specific cellular state conditions, such as the intracellular  $Ca^{2+}$  level, have been developed (Nguyen et al., 2018; Wang et al., 2017). Enhancing these light-activatable tools for various cell-signaling molecules and validation *in vivo* is highly anticipated.

We used Cry2-CIB1 light-dependent dimerizers to develop a robust PA Tet-controlled gene expression system for mammalian cells. This PA-Tet-OFF/ON system had low background, high-fold activation by light, and it can be used in various mammalian cells. Compared with other light-controlled gene expression systems, one unique feature of the PA-Tet-OFF/ON system is the ability to control it via drug application. By systematically changing the applied light intensity and Dox concentration, finer, tunable gene expression can be achieved in this system. In addition, by restricting Dox application in the PA-Tet-ON system, light-controlled gene expression can be conditionally induced during a narrow time window during the course of long-term experiments both *in vitro* and *in vivo*. This dual-control feature of the PA-Tet-OFF/ON system is beneficial for systems biology experiments, in which the timing, amount, and pattern of gene expression must be tightly controlled.

In conclusion, we developed a PA-Tet-OFF/ON system for precise temporal and spatial control of cellular gene expression. The conventional Tet-OFF/ON system is widely used in various research models, such as transgenic animals or expression vectors with TRE (or TetO) regulatory sequences (Das et al., 2016;

Liu et al., 2012b; Madisen et al., 2015); therefore, our PA-controlled TetR regulators will allow the optogenetic manipulation of genes of interest in broad fields of biology.

## STAR★METHODS

Detailed methods are provided in the online version of this paper and include the following:

- KEY RESOURCES TABLE
- CONTACT FOR REAGENT AND RESOURCE SHARING
- EXPERIMENTAL MODEL AND SUBJECT DETAILS
  - Cell culture
  - Mice
  - Neuronal primary culture
  - Mouse brain study
  - Analysis in the subcutaneous tissue
- METHOD DETAILS
  - Constructs
  - Lentivirus packaging
  - Recombinant AAV production
  - Immunofluorescence staining
  - Light source
  - Patterned light application
  - Luciferase assays
  - Live-cell monitoring of luciferase activity
  - Luciferase imaging
  - Characterization of PA-Tet-OFF/ON
- QUANTIFICATION AND STATISTICAL ANALYSIS
  - Image analysis and quantification
  - Estimation of the activation and deactivation kinetics of light-induced gene expression
  - Statistical analysis
- DATA AND SOFTWARE AVAILABILITY

## SUPPLEMENTAL INFORMATION

Supplemental Information includes four figures, six tables, and one video and can be found with this article online at <https://doi.org/10.1016/j.celrep.2018.09.026>.

## ACKNOWLEDGMENTS

We thank all of the members of the Imayoshi lab, the Kageyama lab, and the SK Project for their support. We also are grateful to Mami Matsumoto, Mika Akiyoshi, and Masako Kawano for technical help. This work was supported by the Japan Society for the Promotion of Science (JSPS) Grant-in-Aid for Scientific Research on Young Scientists (A) (JSPS 15H05570, to I.I.), (B) (JSPS 15K18362, to M.Y.), and (B) (JSPS 17K14950, to M.Y.); Grant-in-Aid for Scientific Research on Innovative Area (JSPS 15H01489, to I.I.; JSPS 16H01424, to I.I.; JSPS 16H06529, to I.I.; and JSPS 18H05127, to H.O.); Grant-in-Aid for Scientific Research on Challenging Exploratory Research (JSPS 26640011, to I.I.); Grant-in-Aid for Scientific Research (B) (JSPS 15H04258, to H.O.) from the Ministry of Education, Culture, Sports, Science and Technology of Japan (MEXT); Japan Science and Technology Agency (JST) Precursory Research for Embryonic Science and Technology (PRESTO) program (JPMJPR14F3, to I.I.); and the Core Research for Evolutional Science and Technology (CREST) program (JPMJCR1752, to I.I.). I.I. also expresses appreciation for the support from the Leading Initiative for Excellent Young Researchers program of MEXT, the Uehara Memorial Foundation, the Waksman Foundation of Japan INC, Japan Foundation for Applied Enzymology, the Mitsubishi Foun-

ation, Kowa Life Science Foundation, and the Tokyo Biochemical Research Foundation.

## AUTHOR CONTRIBUTIONS

M.Y. and I.I. conceived the project and designed the experiments. M.Y., S.C.N., and I.I. performed the experiments. Y.S. conducted the data analysis. H.O. produced and provided the AAV vectors. M.Y. and I.I. wrote the manuscript with input from all of the other authors.

## DECLARATION OF INTERESTS

There has been no significant financial support for this work that could have influenced its outcome. A national (Japanese) patent application, “Light-Controllable Tet-Gene Expression System” (2018-163617), has been filed by the JST.

Received: January 6, 2018

Revised: July 27, 2018

Accepted: September 7, 2018

Published: October 9, 2018

## REFERENCES

- Aoki, K., Kondo, Y., Naoki, H., Hiratsuka, T., Itoh, R.E., and Matsuda, M. (2017). Propagating wave of ERK activation orients collective cell migration. *Dev. Cell* 43, 305–317.e5.
- Cambridge, S.B., Geissler, D., Calegari, F., Anastassiadis, K., Hasan, M.T., Stewart, A.F., Huttner, W.B., Hagen, V., and Bonhoeffer, T. (2009). Doxycycline-dependent photoactivated gene expression in eukaryotic systems. *Nat. Methods* 6, 527–531.
- Crefcoeur, R.P., Yin, R., Ulm, R., and Halazonetis, T.D. (2013). Ultraviolet-B-mediated induction of protein-protein interactions in mammalian cells. *Nat. Commun.* 4, 1779.
- Das, A.T., Tenenbaum, L., and Berkhout, B. (2016). Tet-On systems for doxycycline-inducible gene expression. *Curr. Gene Ther.* 16, 156–167.
- Deisseroth, K. (2015). Optogenetics: 10 years of microbial opsins in neuroscience. *Nat. Neurosci.* 18, 1213–1225.
- Giordano, F., Saheki, Y., Idevall-Hagren, O., Colombo, S.F., Pirruccello, M., Milosevic, I., Gracheva, E.O., Bagriantsev, S.N., Borgese, N., and De Camilli, P. (2013). PI(4,5)P(2)-dependent and Ca(2+)-regulated ER-PM interactions mediated by the extended synaptotagmins. *Cell* 153, 1494–1509.
- Gossen, M., and Bujard, H. (1992). Tight control of gene expression in mammalian cells by tetracycline-responsive promoters. *Proc. Natl. Acad. Sci. USA* 89, 5547–5551.
- Guntas, G., Hallett, R.A., Zimmerman, S.P., Williams, T., Yumerefendi, H., Bear, J.E., and Kuhlman, B. (2015). Engineering an improved light-induced dimer (iLID) for controlling the localization and activity of signaling proteins. *Proc. Natl. Acad. Sci. USA* 112, 112–117.
- Habets, P.E., Clout, D.E., Lekanne Deprez, R.H., van Roon, M.A., Moorman, A.F., and Christoffels, V.M. (2003). Cardiac expression of Gal4 causes cardiomyopathy in a dose-dependent manner. *J. Muscle Res. Cell Motil.* 24, 205–209.
- Hallett, R.A., Zimmerman, S.P., Yumerefendi, H., Bear, J.E., and Kuhlman, B. (2016). Correlating in vitro and in vivo activities of light-inducible dimers: a cellular optogenetics guide. *ACS Synth. Biol.* 5, 53–64.
- Han, X., Chow, B.Y., Zhou, H., Klapoetke, N.C., Chuong, A., Rajimehr, R., Yang, A., Baratta, M.V., Winkle, J., Desimone, R., and Boyden, E.S. (2011). A high-light sensitivity optical neural silencer: development and application to optogenetic control of non-human primate cortex. *Front. Syst. Neurosci.* 5, 18.
- Hecht, B., Müller, G., and Hillen, W. (1993). Noninducible Tet repressor mutations map from the operator binding motif to the C terminus. *J. Bacteriol.* 175, 1206–1210.



- Heindorf, M., and Hasan, M.T. (2015). Fluorescent calcium indicator protein expression in the brain using tetracycline-responsive transgenic mice. *Cold Spring Harb. Protoc.* 2015, 689–696.
- Hisatomi, O., and Furuya, K. (2015). A light-regulated bZIP module, photozipper, induces the binding of fused proteins to the target DNA sequence in a blue light-dependent manner. *Photochem. Photobiol. Sci.* 14, 1998–2006.
- Hörner, M., Müller, K., and Weber, W. (2017). Light-responsive promoters. *Methods Mol. Biol.* 1651, 173–186.
- Hughes, R.M., Bolger, S., Tapadia, H., and Tucker, C.L. (2012). Light-mediated control of DNA transcription in yeast. *Methods* 58, 385–391.
- Imayoshi, I., and Kageyama, R. (2014a). bHLH factors in self-renewal, multipotency, and fate choice of neural progenitor cells. *Neuron* 82, 9–23.
- Imayoshi, I., and Kageyama, R. (2014b). Oscillatory control of bHLH factors in neural progenitors. *Trends Neurosci.* 37, 531–538.
- Imayoshi, I., Isomura, A., Harima, Y., Kawaguchi, K., Kori, H., Miyachi, H., Fujiwara, T., Ishidate, F., and Kageyama, R. (2013). Oscillatory control of factors determining multipotency and fate in mouse neural progenitors. *Science* 342, 1203–1208.
- Isomura, A., Ogushi, F., Kori, H., and Kageyama, R. (2017). Optogenetic perturbation and bioluminescence imaging to analyze cell-to-cell transfer of oscillatory information. *Genes Dev.* 31, 524–535.
- Kaberniuk, A.A., Shemetov, A.A., and Verkhusha, V.V. (2016). A bacterial phytochrome-based optogenetic system controllable with near-infrared light. *Nat. Methods* 13, 591–597.
- Kawano, F., Suzuki, H., Furuya, A., and Sato, M. (2015). Engineered pairs of distinct photoswitches for optogenetic control of cellular proteins. *Nat. Commun.* 6, 6256.
- Kawano, F., Okazaki, R., Yazawa, M., and Sato, M. (2016). A photoactivatable Cre-loxP recombination system for optogenetic genome engineering. *Nat. Chem. Biol.* 12, 1059–1064.
- Kawashima, T., Kitamura, K., Suzuki, K., Nonaka, M., Kamijo, S., Takemoto-Kimura, S., Kano, M., Okuno, H., Ohki, K., and Bito, H. (2013). Functional labeling of neurons and their projections using the synthetic activity-dependent promoter E-SARE. *Nat. Methods* 10, 889–895.
- Kennedy, M.J., Hughes, R.M., Peteya, L.A., Schwartz, J.W., Ehlers, M.D., and Tucker, C.L. (2010). Rapid blue-light-mediated induction of protein interactions in living cells. *Nat. Methods* 7, 973–975.
- Kim, J.H., Lee, S.R., Li, L.H., Park, H.J., Park, J.H., Lee, K.Y., Kim, M.K., Shin, B.A., and Choi, S.Y. (2011). High cleavage efficiency of a 2A peptide derived from porcine teschovirus-1 in human cell lines, zebrafish and mice. *PLoS One* 6, e18556.
- Kim, J.Y., Ash, R.T., Ceballos-Diaz, C., Levites, Y., Golde, T.E., Smirnakis, S.M., and Jankowsky, J.L. (2013). Viral transduction of the neonatal brain delivers controllable genetic mosaicism for visualizing and manipulating neuronal circuits in vivo. *Eur. J. Neurosci.* 37, 1203–1220.
- Kim, C.K., Adhikari, A., and Deisseroth, K. (2017). Integration of optogenetics with complementary methodologies in systems neuroscience. *Nat. Rev. Neurosci.* 18, 222–235.
- Konermann, S., Brigham, M.D., Trevino, A., Hsu, P.D., Heidenreich, M., Cong, L., Platt, R.J., Scott, D.A., Church, G.M., and Zhang, F. (2013). Optical control of mammalian endogenous transcription and epigenetic states. *Nature* 500, 472–476.
- Liu, H., Gomez, G., Lin, S., Lin, S., and Lin, C. (2012a). Optogenetic control of transcription in zebrafish. *PLoS One* 7, e50738.
- Liu, X., Ramirez, S., Pang, P.T., Puryear, C.B., Govindarajan, A., Deisseroth, K., and Tonegawa, S. (2012b). Optogenetic stimulation of a hippocampal engram activates fear memory recall. *Nature* 484, 381–385.
- Luker, G.D., Pica, C.M., Song, J., Luker, K.E., and Piwnicka-Worms, D. (2003). Imaging 26S proteasome activity and inhibition in living mice. *Nat. Med.* 9, 969–973.
- Ma, Z., Du, Z., Chen, X., Wang, X., and Yang, Y. (2013). Fine tuning the LightOn light-switchable transgene expression system. *Biochem. Biophys. Res. Commun.* 440, 419–423.
- Madisen, L., Garner, A.R., Shimaoka, D., Chuong, A.S., Klapoetke, N.C., Li, L., van der Bourg, A., Niino, Y., Egolf, L., Monetti, C., et al. (2015). Transgenic mice for intersectional targeting of neural sensors and effectors with high specificity and performance. *Neuron* 85, 942–958.
- Maiuri, P., Rupprecht, J.F., Wieser, S., Rupprecht, V., Bénichou, O., Carpi, N., Coppey, M., De Beco, S., Gov, N., Heisenberg, C.P., et al. (2015). Actin flows mediate a universal coupling between cell speed and cell persistence. *Cell* 161, 374–386.
- Masamizu, Y., Ohtsuka, T., Takashima, Y., Nagahara, H., Takenaka, Y., Yoshikawa, K., Okamura, H., and Kageyama, R. (2006). Real-time imaging of the somite segmentation clock: revelation of unstable oscillators in the individual presomitic mesoderm cells. *Proc. Natl. Acad. Sci. USA* 103, 1313–1318.
- Miyoshi, H. (2004). Gene delivery to hematopoietic stem cells using lentiviral vectors. *Methods Mol. Biol.* 246, 429–438.
- Mizushima, S., and Nagata, S. (1990). pEF-BOS, a powerful mammalian expression vector. *Nucleic Acids Res.* 18, 5322.
- Motta-Mena, L.B., Reade, A., Mallory, M.J., Glantz, S., Weiner, O.D., Lynch, K.W., and Gardner, K.H. (2014). An optogenetic gene expression system with rapid activation and deactivation kinetics. *Nat. Chem. Biol.* 10, 196–202.
- Müller, K., Engesser, R., Metzger, S., Schulz, S., Kämpf, M.M., Busacker, M., Steinberg, T., Tomakidi, P., Ehrbar, M., Nagy, F., et al. (2013a). A red/far-red light-responsive bi-stable toggle switch to control gene expression in mammalian cells. *Nucleic Acids Res.* 41, e77.
- Müller, K., Engesser, R., Schulz, S., Steinberg, T., Tomakidi, P., Weber, C.C., Ulm, R., Timmer, J., Zurbriggen, M.D., and Weber, W. (2013b). Multi-chromatic control of mammalian gene expression and signaling. *Nucleic Acids Res.* 41, e124.
- Nguyen, N.T., He, L., Martinez-Moczygemba, M., Huang, Y., and Zhou, Y. (2018). Rewiring calcium signaling for precise transcriptional reprogramming. *ACS Synth. Biol.* 7, 814–821.
- Nihongaki, Y., Yamamoto, S., Kawano, F., Suzuki, H., and Sato, M. (2015). CRISPR-Cas9-based photoactivatable transcription system. *Chem. Biol.* 22, 169–174.
- Nihongaki, Y., Furuhashi, Y., Otabe, T., Hasegawa, S., Yoshimoto, K., and Sato, M. (2017). CRISPR-Cas9-based photoactivatable transcription systems to induce neuronal differentiation. *Nat. Methods* 14, 963–966.
- Okuno, H., Akashi, K., Ishii, Y., Yagishita-Kyo, N., Suzuki, K., Nonaka, M., Kawashima, T., Fujii, H., Takemoto-Kimura, S., Abe, M., et al. (2012). Inverse synaptic tagging of inactive synapses via dynamic interaction of Arc/Arg3.1 with CaMKII $\beta$ . *Cell* 149, 886–898.
- Pathak, G.P., Strickland, D., Vrana, J.D., and Tucker, C.L. (2014). Benchmarking of optical dimerizer systems. *ACS Synth. Biol.* 3, 832–838.
- Pathak, G.P., Spiltoir, J.L., Höglund, C., Polstein, L.R., Heine-Koskinen, S., Gersbach, C.A., Rossi, J., and Tucker, C.L. (2017). Bidirectional approaches for optogenetic regulation of gene expression in mammalian cells using Arabidopsis cryptochrome 2. *Nucleic Acids Res.* 45, e167.
- Polstein, L.R., and Gersbach, C.A. (2012). Light-inducible spatiotemporal control of gene activation by customizable zinc finger transcription factors. *J. Am. Chem. Soc.* 134, 16480–16483.
- Rajasethupathy, P., Ferenczi, E., and Deisseroth, K. (2016). Targeting neural circuits. *Cell* 165, 524–534.
- Repina, N.A., Rosenbloom, A., Mukherjee, A., Schaffer, D.V., and Kane, R.S. (2017). At light speed: advances in optogenetic systems for regulating cell signaling and behavior. *Annu. Rev. Chem. Biomol. Eng.* 8, 13–39.
- Rost, B.R., Schneider-Warme, F., Schmitz, D., and Hegemann, P. (2017). Optogenetic tools for subcellular applications in neuroscience. *Neuron* 96, 572–603.
- Sano, H., and Yokoi, M. (2007). Striatal medium spiny neurons terminate in a distinct region in the lateral hypothalamic area and do not directly innervate

- orexin/hypocretin- or melanin-concentrating hormone-containing neurons. *J. Neurosci.* **27**, 6948–6955.
- Shimizu-Sato, S., Huq, E., Tepperman, J.M., and Quail, P.H. (2002). A light-switchable gene promoter system. *Nat. Biotechnol.* **20**, 1041–1044.
- Song, C., and Knöpfel, T. (2016). Optogenetics enlightens neuroscience drug discovery. *Nat. Rev. Drug Discov.* **15**, 97–109.
- Strickland, D., Lin, Y., Wagner, E., Hope, C.M., Zayner, J., Antoniou, C., Sosnick, T.R., Weiss, E.L., and Glotzer, M. (2012). TULIPs: tunable, light-controlled interacting protein tags for cell biology. *Nat. Methods* **9**, 379–384.
- Szulc, J., Wiznerowicz, M., Sauvain, M.O., Trono, D., and Aebischer, P. (2006). A versatile tool for conditional gene expression and knockdown. *Nat. Methods* **3**, 109–116.
- Taslimi, A., Zoltowski, B., Miranda, J.G., Pathak, G.P., Hughes, R.M., and Tucker, C.L. (2016). Optimized second-generation CRY2-CIB dimerizers and photoactivatable Cre recombinase. *Nat. Chem. Biol.* **12**, 425–430.
- Uda, Y., Goto, Y., Oda, S., Kohchi, T., Matsuda, M., and Aoki, K. (2017). Efficient synthesis of phycocyanobilin in mammalian cells for optogenetic control of cell signaling. *Proc. Natl. Acad. Sci. USA* **114**, 11962–11967.
- Voon, D.C., Subrata, L.S., Baltic, S., Leu, M.P., Whiteway, J.M., Wong, A., Knight, S.A., Christiansen, F.T., and Daly, J.M. (2005). Use of mRNA- and protein-destabilizing elements to develop a highly responsive reporter system. *Nucleic Acids Res.* **33**, e27.
- Wang, X., Chen, X., and Yang, Y. (2012). Spatiotemporal control of gene expression by a light-switchable transgene system. *Nat. Methods* **9**, 266–269.
- Wang, W., Wildes, C.P., Pattarabanjird, T., Sanchez, M.I., Guber, G.F., Matthews, G.A., Tye, K.M., and Ting, A.Y. (2017). A light- and calcium-gated transcription factor for imaging and manipulating activated neurons. *Nat. Biotechnol.* **35**, 864–871.
- Wu, L., and Yang, H.Q. (2010). CRYPTOCHROME 1 is implicated in promoting R protein-mediated plant resistance to *Pseudomonas syringae* in *Arabidopsis*. *Mol. Plant* **3**, 539–548.
- Yazawa, M., Sadaghiani, A.M., Hsueh, B., and Dolmetsch, R.E. (2009). Induction of protein-protein interactions in live cells using light. *Nat. Biotechnol.* **27**, 941–945.
- Yu, X., Liu, H., Klejnot, J., and Lin, C. (2010). The cryptochrome blue light receptors. *Arabidopsis Book* **8**, e0135.
- Zhu, P., Aller, M.I., Baron, U., Cambridge, S., Bausen, M., Herb, J., Sawinski, J., Cetin, A., Osten, P., Nelson, M.L., et al. (2007). Silencing and un-silencing of tetracycline-controlled genes in neurons. *PLoS One* **2**, e533.

## STAR★METHODS

### KEY RESOURCES TABLE

REAGENT or RESOURCE	SOURCE	IDENTIFIER
<b>Antibodies</b>		
Mouse monoclonal anti-MAP2	Sigma-Aldrich	Cat# M4403; RRID: AB_477193
Rabbit polyclonal anti-GFP	ThermoFisher	Cat# A11122; RRID: AB_221569
Mouse monoclonal anti-NeuN	Millipore	Cat# MAB377; RRID: AB_2298772
<b>Bacterial and Virus Strains</b>		
AAV2/DJ8-CAG-FLAG-TetR (I194T, 1–206)-CIBN (without NLS)-T2A-mCherryNLS	This paper	N/A
AAV2/DJ8-CAG-NLS-attached Cry2 PHR (L348F)-p65 AD N-terminal fusion	This paper	N/A
AAV2/DJ8-TRE3G-luc2-Hes1 3' UTR	This paper	N/A
pAAV-DJ/8 and pHelper packaging vectors	Cell Biolabs	Cat# VPK-430-DJ-8
CSII-EF-PA-Tet-OFF/ON	This paper	N/A
CSII-EF-PA-Tet-OFF/ON-IRES2-Bsd	This paper	N/A
CSII-EF-PA-Tet-OFF/ON-IRES2-mCherryNLS	This paper	N/A
CSII-CAG-PA-Tet-OFF/ON	This paper	N/A
CSII-TRE3G-NLS-Ub-luc2-Hes1 3' UTR	This paper	N/A
CSII-TRE3G-luc2-Hes1 3' UTR	This paper	N/A
<b>Chemicals, Peptides, and Recombinant Proteins</b>		
Matrigel Basement Membrane Matrix	Becton Dickinson	Cat# 356234
GlutaMAX-I Supplement	ThermoFisher	Cat# 35050061
Insulin from bovine pancreas	Sigma-Aldrich	Cat# I5500-100MG
GS21 Neural Supplement	GlobalStem	Cat# GSM-3100
FBS Hyclone	ThermoFisher	Cat# SH30071.03
Cytosine $\beta$ -D-arabinofuranoside hydrochloride crystalline (AraC)	Sigma-Aldrich	Cat# C6645
D-luciferin sodium salt	Nacalai Tesque	Cat# 01493-85
Blasticidin S HCl	ThermoFisher	Cat# R21001
AAVpro extraction solution	TAKARA	Cat# 6235
OptiPrep	Alere Technologies AS	Cat# 1114542
Lipofectamine LTX	ThermoFisher	Cat# 15338100
Polyethylenimine	Polysciences	Cat# 24765-2
<b>Critical Commercial Assays</b>		
Luciferase Assay System	Promega	Cat# E1501
<b>Deposited Data</b>		
Raw and analyzed data	This paper	<a href="https://doi.org/10.17632/v3fn547spz.1">https://doi.org/10.17632/v3fn547spz.1</a>
<b>Experimental Models: Cell Lines</b>		
HEK293T	ATCC	Cat# CRL-3216
Eph4	ATCC	Cat# CRL-3071
<b>Experimental Models: Organisms/Strains</b>		
TRE-GFP transgenic mouse strain	<a href="#">Sano and Yokoi, 2007</a>	RBRC02340
<b>Recombinant DNA</b>		
pEF-mCherryNLS	<a href="#">Imayoshi et al., 2013</a>	N/A
pEF-luc2	This paper	N/A
pLVPT-tTR-KRAB	<a href="#">Szulc et al., 2006</a>	Addgene, #11642
pEF-hGAVPO	<a href="#">Imayoshi et al., 2013; Wang et al., 2012</a>	N/A

(Continued on next page)

### Continued

REAGENT or RESOURCE	SOURCE	IDENTIFIER
pEF-BOS	<a href="#">Mizushima and Nagata, 1990</a>	N/A
TREtight-Ub-Eluc	This paper	N/A
CSII-EF-MCS	<a href="#">Imayoshi et al., 2013</a> ; <a href="#">Miyoshi, 2004</a>	N/A
CSII-EF-MCS-IRES2-Bsd	<a href="#">Imayoshi et al., 2013</a> ; <a href="#">Miyoshi, 2004</a>	N/A
CSII-EF-MCS-IRES2-mCherryNLS	<a href="#">Imayoshi et al., 2013</a> ; <a href="#">Miyoshi, 2004</a>	N/A
CSII-CAG-MCS	<a href="#">Imayoshi et al., 2013</a> ; <a href="#">Miyoshi, 2004</a>	N/A
pAAV-CAG-ArchT-GFP	<a href="#">Han et al., 2011</a>	Addgene plasmid #29777
pFBAAV	<a href="#">Kawashima et al., 2013</a>	N/A
pTet-OFF advanced vector	Clontech/TAKARA	Cat# 631070
Tet-ON 3G inducible expression system	Clontech/TAKARA	Cat# 631168
pEF-FLAG-tTA-Ad	This paper	N/A
pEF-FLAG-TetON3G	This paper	N/A
pEF-PA-Tet-OFF/ON	This paper	N/A
Software and Algorithms		
MetaMorph	Universal Imaging	Version 7.8.10.0
ImageJ software and custom plug-ins	<a href="#">Imayoshi et al., 2013</a> ; <a href="#">Isomura et al., 2017</a>	N/A
Prism software	GraphPad Software	Version 5.0
MATLAB	MathWorks	Version 9.2
Curve Fitting Toolbox	MathWorks	version 3.5.5
Signal Processing Toolbox	MathWorks	version 7.4

### CONTACT FOR REAGENT AND RESOURCE SHARING

Further information and requests for resources and reagents should be directed to and will be fulfilled by the Lead Contact, Itaru Imayoshi ([imayoshi.itaru.2n@kyoto-u.ac.jp](mailto:imayoshi.itaru.2n@kyoto-u.ac.jp)).

### EXPERIMENTAL MODEL AND SUBJECT DETAILS

Animal handling and experimental protocols were approved by the Animal Care Committee of Kyoto University (permit numbers: Med Kyo 14126, Med Kyo 15503, Med Kyo 16216, Med Kyo 17061, and Lif-K18018) and conformed to all relevant regulatory standards.

#### Cell culture

HEK293T and Eph4 cells (American Type Culture Collection [ATCC]) were cultured at 37°C and 5% CO<sub>2</sub> in Dulbecco's Modified Eagle Medium (DMEM; Nacalai Tesque) supplemented with 10% fetal bovine serum (FBS; Hyclone; ThermoFisher) and 100 units/mL penicillin and 100 mg/mL of streptomycin (Nacalai Tesque). HEK293T and Eph4 cells were passaged using 0.05% and 0.25% Trypsin/EDTA (GIBCO), respectively.

#### Mice

Male or female 10- to 14-week-old TRE-GFP transgenic mice ([Sano and Yokoi, 2007](#)) were used for the analysis in the adult brain. ICR embryos and pups (Japan SLC, Shizuoka, Japan) were used for the analysis in the neuronal primary culture, and embryonic or early-postnatal brain. Male or female 8- to 20-week-old adult ICR mice (Japan SLC, Shizuoka, Japan) were used for the analysis in the subcutaneous tissue. The mice were group housed in a standard laboratory environment, maintained on a 14-h light/10-h dark cycle at a constant temperature (23–24°C) and relative humidity (40%–50%). Food (pellets; Japan SLC) and water were provided *ad libitum*.

#### Neuronal primary culture

Hippocampal neurons were prepared from the CA1/CA3/dentate gyrus regions of the hippocampus of 1-day-old (P1) mouse pups essentially as described previously ([Okuno et al., 2012](#)) with minor modifications. Briefly, the dissociated cells were plated on Matrigel (Becton Dickinson)-coated coverslips (Assistant, Karl Hecht GmbH & Co, Germany), and cultured in minimal essential medium (MEM) supplemented with 1 mM GlutaMAX-I (ThermoFisher), 25 µg/mL insulin (Sigma-Aldrich), 2% GS21 Neural Supplement (GlobalStem), and 5% FBS (Hyclone; ThermoFisher). Glial proliferation was suppressed by adding 4 µM cytosine arabinoside (Sigma-Aldrich) to the medium 24–48 h after plating.

## Mouse brain study

For the validation of the PA-Tet system in the neural stem or progenitor cells of the developing mouse brain, the elongation factor promoter (pEF)-mCherryNLS (NLS: nuclear localization signal), pEF-PA-Tet-OFF and CSII-TRE3G-NLS-Ub-luc2-Hes1 3' untranslated region (UTR) plasmids were mixed at a 2:9:9 ratio, and co-transfected into E14.5 dorsal telencephalon progenitors by ex utero electroporation (Imayoshi et al., 2013). Plasmid DNA (2.5  $\mu\text{g}/\mu\text{l}$ ) was microinjected into a telencephalic ventricle, and ex utero electroporation (6 pulses, 50 mV, square wave generator (CUY21, BEX), 5-mm paddle electrodes) was performed for transfection of plasmids into neural stem or progenitor cells at the ventricular surface of the neocortex. Brains were immediately dissected, embedded in 3% low-melting point agarose, cut into 250- $\mu\text{m}$  organotypic slices with a vibratome (VT1000; Leica), transferred to 12-mm well culture insert (Millicell, PICM01250, Merck), and cultured in slice culture medium, as described previously (Imayoshi et al., 2013). Slices were incubated at 37°C, 5% CO<sub>2</sub> under periodic blue-light irradiation.

For the validation of the PA-Tet system in neurons of the adult brain, mice were subjected to stereotactic virus injections using pulled glass micropipettes, as described previously (Kawashima et al., 2013; Sano and Yokoi, 2007). The mice (10–14 weeks old) were anesthetized with 440 mg/kg chloral hydrate (Tokyo Chemical Industry) by intraperitoneal injection. Petrolatum was applied to both eyes to prevent dryness, and the skin on the head was treated with hair-removal cream. The mice were then fixed to a small-animal stereotactic device (David Kopf Instruments). The head skin was cut at the midline, and the periosteum was removed using a surgical knife. The skull was thinned with a drill, and a small craniotomy was made using a 27-gauge needle. The virus was injected through a pulled glass micropipette connected to a Hamilton syringe (Hamilton Company), which was pumped using a syringe pump device (World Precision Instruments). The stereotactic injections were administered to the following tissue at the appropriate coordinates: the dentate gyrus of the hippocampus (A/P  $-1.94$  mm, M/L  $\pm 1.3$  mm from the bregma, D/V  $-1.82$  mm from the pial surface). The two AAV vectors were co-transduced at a 1:1 ratio: AAV2/DJ8-CAG-FLAG-TetR (I194T, 1–206)-CIBN (without NLS)-T2A-mCherryNLS and AAV2/DJ8-CAG-NLS-attached Cry2 PHR (L348F)-p65 AD (p65 AD; residues 286–550 of human p65 transcriptional activation domain) N-terminal fusion. The viral solution was injected at a rate of 0.1  $\mu\text{l}/\text{min}$  in a volume of 0.5–1.5  $\mu\text{l}$ , and after the injection, the pipette was held in place for an additional 10 min before removal. After the removal of the micropipette, the skin incision was sutured and treated with antibiotic cream, and an analgesic was injected subcutaneously to relieve post-surgical pain. The post-injection animals were bred normally for 2 weeks before blue light exposure.

For the AAV transduction to mouse pup brains, anesthetized ICR mice at postnatal day 0 or 1 were placed on the custom-made stage. The three AAV vectors were injected into the lateral ventricle of the right hemisphere (Kim et al., 2013) at a 1:1:1 ratio: AAV2/DJ8-CAG-FLAG-TetR (I194T, 1–206)-CIBN (without NLS)-T2A-mCherryNLS, AAV2/DJ8-CAG-NLS-attached Cry2 PHR (L348F)-p65 AD N-terminal fusion, and AAV2/DJ8-TRE3G-luc2-Hes1 3' UTR.

Light stimulation was started 15 days after AAV transduction. For the hippocampus-light illumination of the adult mice, awake and freely moving mice were stimulated using a blue LED (PlexBright, Plexon) connected to the optical implant via fiber patch cables and a rotary joint at an intensity of 85.6 W/m<sup>2</sup>, duty cycle of 1.6% (1 s pulses at 0.016 Hz) for 12 h. After the blue light exposure, mice were immediately sacrificed and perfused. The dissected brains were subjected to immunohistochemistry. For the pup brain illumination, anesthetized mice were stimulated using a blue LED (PlexBright, Plexon) through an optical fiber. The blue light (40 W/m<sup>2</sup>; 1 s pulse every 15 s; 3 h duration)-irradiated right brains were immediately extracted, lysed, and their luciferase activity determined. For Dox pulse treatment, 0.1 mg/g body weight of Dox was given by a single intraperitoneal injection (Zhu et al., 2007; Heindorf and Hasan, 2015).

## Analysis in the subcutaneous tissue

2–5  $\times 10^6$  cells of the stable cell clone of PA-Tet-OFF-transduced Eph4 cells were engrafted into the subcutaneous tissue of the adult mouse back. For bioluminescence detection, the animals were imaged by a CCD camera (iXon3, Andor Instruments, Belfast) 24 h after the injection of Eph4 cells. Prior to imaging, 200 mg/g body weight of luciferin (Nacalai Tesque) was intraperitoneally, subcutaneously and intramuscularly injected. The engrafted regions were illuminated with blue light (200 W/m<sup>2</sup>; 1-min). Dox (0.1 mg/g body weight) was injected intraperitoneally 1 h before illumination. To correct the luciferase signal changes caused by the fluctuation of the luciferin substrate in the mouse body, we engrafted Eph4 cells transfected with pEF-luc2 expression vector to control mice, which were imaged together with the mice engrafted with the PA-Tet-OFF-transduced Eph4 cells. Luminescence data of the control mice were used for the correction of the light-induced transcription in the transplanted PA-Tet-OFF-transduced Eph4 cells. The mean values of the luminescence signals between 30 min and 60 min after blue light illumination were plotted in the bar graphs.

## METHOD DETAILS

### Constructs

For functional screening of PA-Tet-OFF candidate constructs, sequences encoding the DNA binding, dimerization, and Tet binding domains of TetR (residues 1–206), and the transcriptional activation domain of p65 were amplified using pLVPT-tTR-KRAB (Addgene plasmid #11642) (Szulc et al., 2006) and pEF-hGAVPO (Imayoshi et al., 2013; Wang et al., 2012), respectively. The optimized mammalian codon sequences encoding the derivatives of Cry2 (Cry2 PHR, Cry2 PHR [L348F], Cry2 535, and Cry2 535 [L348F]), and CIB1 and



its derivatives (CIB1 without nuclear localization sequences [NLS], CIBN, CIBN without NLS sequences, and CIB81), were synthesized by FASMAC (Kanagawa, Japan) (Hallett et al., 2016; Kennedy et al., 2010; Taslimi et al., 2016).

To validate the flexible linker sequences, the sequence derived from tTA-Ad (pTet-OFF Advanced; Clontech/TAKARA) with an S2A point mutation was used. The amino acid sequence encoded by tTA-Ad (S2A, 1–206) was identical to that of TetR (residues 1–206). Using these sequences, TetR (residues 1–206) or p65 AD was fused to Cry2- or CIB1 derivatives, and additional point mutations, the NLS, T2A, or FLAG tag sequences were introduced/attached by conventional overlap polymerase chain reaction (PCR) extension, restriction enzyme digestion, and ligation methods. These constructs were cloned into expression vector plasmids with the human elongation factor 1a promoter sequence and polyadenylation sequences (pEF-BOS) and its derivatives (Mizushima and Nagata, 1990). All prepared constructs were verified by DNA sequencing.

To generate PA-Tet-ON candidate constructs, we synthesized TetR sequences with the following reverse phenotype mutations: rtTA (E71K, D95N, L101S, G102D), S2 (E19G, A56P, D148E, H179R), M2 (S12G, E19G, A56P, D148E, H179R), V10 (E19G, A56P, F67S, F86Y, D148E, R171K, H179R), V16 (V9I, E19G, A56P, F67S, F86Y, D148E, R171K, H179R) (Das et al., 2016). Then, these sequences were replaced with the TetR sequence of the PA-Tet-OFF plasmids. *Pyrearinus termitilluminans* Emerald luciferase (Eluc; TOYOBO) was used to generate a reporter plasmid for PA-Tet-OFF/ON activity. The N terminus of Eluc was fused to one copy of a mutant ubiquitin (G76V) for rapid degradation to prevent long-term accumulation of the reporter in cells (Masamizu et al., 2006). The Ub-Eluc coding sequence was inserted into the TREtight plasmid (Clontech/TAKARA).

In the plasmid constructions for lentivirus vectors, coding sequences of the PA-Tet constructs were inserted into multiple cloning sites of CSII-EF-MCS, CSII-EF-MCS-IRES2-Bsd, CSII-EF-MCS-IRES2-mCherryNLS, or CSII-CAG-MCS plasmids (Imayoshi et al., 2013; Miyoshi, 2004). *Bsd* is the resistance gene for blasticidin. CSII-EF-MCS was digested with *AgeI* to remove the elongation factor (EF) promoter, and the TRE3G sequence (Clontech/TAKARA) and the 3' UTR of the mouse *Hes1* gene were cloned in the opposite orientation to long terminal repeat (LTR)-mediated transcription. An Ub-NLS-luc2 or luc2 coding sequence was inserted immediately after the TRE3G sequence.

In the plasmid constructions for adeno-associated virus (AAV) vectors, the coding sequence for FLAG-TetR (I194T, 1–206)-CIBN (without NLS)-T2A-mCherryNLS or NLS-attached Cry2 PHR (L348F)-p65 AD N-terminal fusion constructs was inserted into the multiple cloning site of pAAV-CAG-ArchT-GFP (Addgene plasmid #29777) (Han et al., 2011) by removing the ArchT-GFP sequence with *BamHI*- and *EcoRI*-digestion. The TRE-controlled luciferase reporter plasmid was constructed in the pFBAAV vector (Kawashima et al., 2013) by inserting the TRE3Gs sequences, cDNAs for luc2 with the *Hes1* 3' UTR sequence, to generate inverted terminal repeats (ITR)-flanked expression cassettes. (pFBAAV-TRE3G-luc2-*Hes1* 3' UTR). Further details on the cloning strategy, and complete sequences for the plasmids used in this study are available upon request.

### Lentivirus packaging

Lentiviral particles were produced via calcium phosphate cotransfection or lipofection of HEK293T cells with packaging plasmids using a previously described procedure (Imayoshi et al., 2013; Miyoshi, 2004). Supernatants were collected starting at 24 h after transfection for 36 h and concentrated by centrifugation at 6,000 *g* for 16 h. The resulting viral pellet was resuspended in phosphate-buffered saline (PBS) or saline at 1/100 to 1/500 of the original volume, and the viral aliquot was then frozen. Viral titers were approximately  $10^{8-9}$  infectious units/mL. Cultured cells were infected by purified lentiviral particles with a multiplicity of infection (MOI) = ~10–20. Transduced cells were selected by blasticidin S (2  $\mu$ g/mL; ThermoFisher) for the lentivirus vectors co-expressing *Bsd*, or by fluorescence-activated cell sorting for lentivirus vectors co-expressing mCherry.

### Recombinant AAV production

Serotype DJ/8 AAVs were produced in HEK293T cells by transfecting ITR-containing AAV vectors together with the packaging vectors pAAV-DJ/8 and pHelper (Cell Biolabs, Inc.). Recombinant AAV particles were collected from transfected cells using an extraction kit (AAVpro extraction solution, TaKaRa Bio). Recovered AAV particles were further purified using discontinuous iodixanol gradients (OptiPrep, Alere Technologies AS) with ultracentrifugation, and concentrated in PBS by ultrafiltration. Viral titers of the purified AAVs were measured by qPCR and adjusted to  $2 \sim 10 \times 10^{12}$  genome copies per milliliter (gc/ml).

### Immunofluorescence staining

Cells or tissues were washed with PBS and fixed with 4% paraformaldehyde/PBS for 20 min at room temperature. Fixed cells were washed with PBS, then blocked and permeabilized with 5% normal donkey serum (NDS) and 0.1% Triton X-100/PBS at room temperature for 20 min, incubated with primary antibodies diluted in PBS containing 1% NDS overnight at 4°C, washed with PBS, and then incubated with regular secondary antibodies conjugated to Alexa 405, Alexa 488, or Alexa 594 (Invitrogen) for 1 h at room temperature. Stained cells or tissues were photographed with an LSM510 or LSM780 confocal microscope (Zeiss). The following primary antibodies were used; mouse monoclonal anti-MAP2 (M4403, Sigma-Aldrich), rabbit polyclonal anti-GFP (A11122, ThermoFisher), and mouse monoclonal anti-NeuN (MAB377, Millipore) antibodies.

### Light source

For blue-light irradiation of cultured cells in CO<sub>2</sub> incubators, we used an LED light source: LEDB-SBOXH (OptoCode). For blue-light illumination under the microscope (except for patterned light application), blue light was generated by a pE-2 LED excitation system

(CoolLED) equipped with 470-nm LAM. To apply light to neural cells in the brain, blue light was delivered by a pen light (465nm Handy Blue Pro Plus; RelyOn) or PlexBright (465 nm, Plexon).

### Patterned light application

A Mosaic 3 pattern illuminator (Andor) coupled to a blue-light-emitting diode (X-Cite® 120LED; Excelitas Technologies) was attached to the microscope and used for light delivery through the objective lens.

### Luciferase assays

Luciferase activity of the lysed cells was assayed according to the manufacturer's protocol (Luciferase Assay System; Promega).

### Live-cell monitoring of luciferase activity

Luminescence signals at the population level were recorded by a live-cell monitoring system (CL24B-LIC/B; Churitsu Electric Corp.) equipped with a high-sensitive photomultiplier tube (PMT) and an LED blue light source (LEDB-SBOXH; OptoCode). Cells were plated on black 24-well plates with 1 mM luciferin-containing medium, and photon-counting measurements were performed.

### Luciferase imaging

Cells were plated on 35-mm glass-base dishes at 50%–60% confluence and incubated at 37°C and 5% CO<sub>2</sub>. One mM luciferin was then added to the culture medium. Bioluminescence images were acquired by an upright microscope (IX83; Olympus) with a 20 × or 40 × dipping objective. Digital images were acquired using a cooled CCD camera (iKon-M DU934P-BV; Andor). The filters and camera control were adjusted automatically using software (MetaMorph®; Universal Imaging Corp.). Stray light was eliminated by turning off the electric system. The imaging system was used in a dark room.

### Characterization of PA-Tet-OFF/ON

For functional screening of the PA-Tet-OFF candidate constructs, HEK293T cells were plated at  $5 \sim 9 \times 10^4$  cells/well on a 24-well plate, and cultured for 24 h at 37°C in 5% CO<sub>2</sub>. The cells were then transfected with Lipofectamine® LTX (ThermoFisher) or polyethylenimine (Polysciences, Inc.) according to the manufacturer's protocols. Three plasmids were co-transfected at a 25:25:8 ratio: pEF-TetR (1–206) fused with Cry2/CIB-derivative, pEF-p65 AD fused with Cry2/CIB-derivative, and pTREtight-Ub-ELuc reporter. The total amount of DNA was 0.58 µg/well. Forty-eight hours after transfection, the cells were exposed to blue light (7.2 W/m<sup>2</sup>; 2 s pulse every 1 min) for 3 h. Thereafter, cells were lysed and their luciferase activity was measured with a plate reader (ARVO X3; PerkinElmer). Control cells were kept in the dark after plasmid transfection. For the analysis of constructs having the T2A sequence, the expression vector, pBluescript plasmid, and the reporter were mixed at a 25:25:8 ratio and transfected. The pBluescript plasmid was used to adjust the total amount of transfected DNA.

To analyze the relationship between the intensity of light exposure and the level of induced gene expression, stable Eph4-cell clones transduced with PA-Tet-OFF and TRE3G-Ub-NLS-luc2-Hes1 3' UTR lentivirus vectors were plated at  $5 \sim 9 \times 10^4$  cells/well on a 24-well plate, cultured for 24 h, and assayed in a manner identical to that of the candidate construct screening. Blue light (7.2 W/m<sup>2</sup>; 2 s pulse every 1 min) was applied for 3 h to cells at the following irradiances: 0, 1.7, 3.5, 5.5, and 7.0 W/m<sup>2</sup>.

For comparing maximum induced gene expression levels between the PA-Tet and chemically regulated Tet-system, the following plasmids were used: pEF-FLAG-tTA-Ad and pEF-FLAG-TetON3G. tTA-Ad and TetON3G sequences were PCR amplified from the pTet-OFF advanced vector (Cat. #631070) and Tet-ON 3G inducible expression system (Cat. #631168) (Clontech/TAKARA), respectively. HEK293T cells were plated on a 24-well plate at  $0.8 \sim 1 \times 10^5$  cells/well and transfected. Twelve hours after transfection, the cells were exposed to blue light (7.2 W/m<sup>2</sup>; 1 s pulse every 30 s) for 36 h. 500 ng/mL of Dox was added to the cell culture medium.

To analyze the relationship between Dox concentration and the level of induced gene expression, HEK293T cells were plated on a 24-well plate at  $5 \sim 9 \times 10^4$  cells/well, transfected, and assayed similar to the candidate construct screening. Dox was applied to cells at the following concentrations: 0, 1, 7.5, 15, 20, 50, 100 and 500 ng/mL for PA-Tet-OFF constructs and 0, 10, 15, 20, 30, 35, 40, 50, 75, 100, 250, 500, 750 and 1000 ng/mL for PA-Tet-ON constructs. Blue light (7.2 W/m<sup>2</sup>; 2 s pulse every 1 min) was shone on the cells for 3 h.

To examine dual control by light intensity and Dox concentration, stable cell clones transduced with PA-Tet-ON and TRE3G-Ub-NLS-luc2-Hes1 3' UTR lentivirus vectors were plated at  $1 \times 10^5$  cells/well on a 24-well plate, and cultured for 24 h. Dox was applied to cells at the following concentrations: 0, 50, 75, 87.5, 92.5, 100, 250, and 500 ng/mL. Blue light (7.2 W/m<sup>2</sup>; 2 s pulse every 1 min) was used for 3 h at the following irradiances: 0, 1.8, 3.6, 5.9, and 7.1 W/m<sup>2</sup>.

To examine the temporal characteristics of PA-Tet-OFF/ON, transfected HEK293T cells or lentivirus-transduced Eph4 cells were used. Cells were plated at  $1 \times 10^4$  cells/well on black 24-well plates and exposed to blue light (7.2 W/m<sup>2</sup>) for 1~2 min. Luminescence signals at the population level were recorded by a live-cell monitoring system (CL24B-LIC/B; Churitsu Electric Corp.). For the analysis of PA-Tet-ON system, Dox (1,000 ng/mL) was supplied in the cell culture medium.

To determine if PA-Tet-ON was conditionally activated by adding and removing Dox in long-term cell culture, lentivirus-transduced Eph4 cells were plated at  $3 \times 10^3$  cells/well in black 24-well plates. In the Dox washout procedure, cells were washed once with PBS. Dox was applied to cells at 1,000 ng/mL 1 h before illumination. Cells were exposed to blue light (7.2 W/m<sup>2</sup>) for 3 min.

To examine the ability of the PA-Tet system to spatially control gene expression in the targeted cells, lentivirus-transduced Eph4 cells were plated on 35-mm glass-base dishes (Cat. #3910-035; IWAKI) at 50%–60% confluence and incubated at 37°C and 5% CO<sub>2</sub> in the chamber stage of the microscope before illumination. Patterned light was generated by the MOSAIC 3 device (Andor) and applied to the cells. Light (10-ms pulse) was applied to cells 50 times, and temporal changes in luminescence signals were acquired. When the blue light source power was set to 100%, and 200 pixel × 200 pixel regions were targeted through the 40 × objective lens (Olympus UApo 40 × Oil Iris3/340; NA was modified to 0.55), the measured light energy was 1.3 W/m<sup>2</sup>.

## QUANTIFICATION AND STATISTICAL ANALYSIS

### Image analysis and quantification

Image analysis was performed using ImageJ software and custom plug-ins (Imayoshi et al., 2013; Isomura et al., 2017). The custom-written code for the ImageJ plug-ins used in this study is available upon request. To analyze bioluminescence imaging sequence files, a “spike-noise filter” was applied to a stack file to remove noise signals caused by cosmic rays. CCD readout noise was also removed by a “temporal background reduction filter.” In this normalization procedure, the background value measured outside of the imaging regions for each time frame was subtracted from the signal intensity. “Circadian gene expression” (CGE) (<http://bigwww.epfl.ch/sage/soft/circadian/>) tracked individual cells and quantified bioluminescence signals. Nuclear localized mCherry was co-expressed and used to detect and track moving cells. The average signal intensity inside the nucleus was measured, illustrated, and analyzed by Prism® 5.0 software (GraphPad Software).

### Estimation of the activation and deactivation kinetics of light-induced gene expression

The half-lives of the switch-on/off kinetics of light-induced gene expression in the PA-Tet-OFF and PA-Tet-ON systems were determined using the following 3 steps. First, each waveform was detrended to remove the linear trends of activities independent of photostimulation. In the detrend processing, a linear regression was performed on data points fewer than median absolute deviation of the waveform, then values predicted by the regression were subtracted from all points of the waveform. Second, event epochs induced by photostimulation were estimated by comparing each value in the waveform with a probabilistic threshold. In the probabilistic threshold, random numbers with the same length of the waveform vector were generated from a Gaussian distribution. The probabilistic threshold was generated by the same method in all analyses. Each value in the waveform was compared with that in the threshold at the corresponding time point. This process was iterated 100 times, and time points when the probability exceeding the threshold was more than 50% were treated as events (i.e., light-induced gene expression). Finally, the values of  $\tau_{on}$  and  $\tau_{off}$  were estimated as the duration from the beginning of the event epoch to the peak, and the peak to the end of the event epoch. The half-lives of the switch-on/off kinetics of the light-induced gene expression were calculated with the  $\tau_{on}$  and  $\tau_{off}$  values.

### Statistical analysis

Statistical analyses were performed with Prism® 5.0 software (GraphPad). P values less than 0.05 were considered significant. Statistical methods used in the analysis are described in the figure legends.

## DATA AND SOFTWARE AVAILABILITY

Requests for custom scripts and raw data can be directed to the Lead Contact, Itaru Imayoshi ([imayoshi.itaru.2n@kyoto-u.ac.jp](mailto:imayoshi.itaru.2n@kyoto-u.ac.jp)). Raw and analyzed data, and custom scripts were deposited to Mendelay Data (<https://doi.org/10.17632/v3fn547spz.1>).